TURUN
YLIOPISTO
UNIVERSITY
OF TURKU

UPCONVERTING NANOPARTICLES IN ULTRASENSITIVE DETECTION

of cardiac troponin I

Kirsti Raiko

TURUN YLIOPISTON JULKAISUJA – ANNALES UNIVERSITATIS TURKUENSIS
SARJA – SER. F OSA – TOM. 24 | TECHNICA – INFORMATICA | TURKU 2023

TURUN
YLIOPISTO
UNIVERSITY
OF TURKU

UPCONVERTING NANOPARTICLES IN ULTRASENSITIVE DETECTION

of cardiac troponin I

Kirsti Raiko

TURUN YLIOPISTON JULKAISUJA – ANNALES UNIVERSITATIS TURKUENSIS
SARJA – SER. F OSA – TOM. 24 | TECHNICA – INFORMATICA| TURKU 2023

University of Turku

Faculty of Technology
Department of Life Technologies
Molecular Biotechnology and Diagnostics
Doctoral programme in Technology

Supervised by

Professor Tero Soukka, PhD
Department of Life Technologies
University of Turku
Turku, Finland

Teppo Salminen, PhD
Uniogen Oy
Turku, Finland

Iida Martiskainen, PhD
Department of Life Technologies
University of Turku
Turku, Finland

Satu Lahtinen, PhD
Department of Life Technologies
University of Turku
Turku, Finland

Reviewed by

Docent Harri Siitari, PhD
Turku, Finland

Professor Laura Anfossi, PhD
Department of Chemistry
University of Turin,
Turin, Italy

Opponent

Senior Research Associate
Thomas Hirsch, PhD
Institute of Analytical Chemistry
University of Regensburg
Regensburg, Germany

The originality of this publication has been checked in accordance with the University of Turku quality assurance system using the Turnitin OriginalityCheck service.

Cover Image: Transmission electron microscopy image of $NaYF_4$: Yb^{3+}, Er^{3+} - nanoparticles taken by Kirsti Raiko, colour manipulated by Saara Kuusinen

ISBN 978-951-29-9385-7 Print
ISBN 978-951-29-9386-4 PDF
ISSN 2736-9390 (Painettu/Print)
ISSN 2736-9684 (Sähköinen/Online)
Painosalama, Turku, Finland 2023

It seems to me that the natural world is the greatest source of excitement;
the greatest source of visual beauty, the greatest source of intellectual interest.
It is the greatest source of so much in life that makes life worth living.

Sir David Attenborough

UNIVERSITY OF TURKU
Faculty of Technology
Department of Life Technologies
Biotechnology
KIRSTI RAIKO: Upconverting nanoparticles in ultrasensitive detection of cardiac troponin I
Doctoral Dissertation, 133 pp.
Doctoral Programme in Technology
September 2023

ABSTRACT

Development of high-sensitivity immunoassays is a continuous interest in medical diagnostics, especially in the case of such diseases where higher sensitivity analyte measurements improve the prognosis of treatment. One such analyte is cardiac troponin I, used for detection of cardiac events. One of the key factors determining immunoassay sensitivity is the reporter, which labels the analytes in the assays and produces the measurable signal. Upconverting nanoparticles (UCNPs) are promising candidates for reporters in sensitive immunoassays. Their unique ability to convert near-infrared light into higher energy visible light by stacking photons, producing emission exhibiting anti-Stokes shift. As no other natural materials are capable of the process, measurement of UCNPs can be designed to completely dismiss any background signal originating from autofluorescence. However, reaching the maximal sensitivity they theoretically enable has been hindered by their tendency to non-specifically bind to solid surfaces in assays and to each other, forming nanoparticle clusters of varying sizes. The extent of these tendencies has been linked to the surface chemistry of the UCNPs.

The aim of this thesis was to study the surface chemistry of UCNPs and apply them as reporters in different immunoassay technologies for detection of cTnI. During the research, surface coating of UCNPs with poly(acrylic acid) was studied and successfully improved, leading to reduced non-specific binding and cluster formation tendency. The performance of the UCNPs with the novel surface was compared to other surface chemistry approaches in microtiter plate assays utilizing either analog or digital readout method, and a lateral flow assay.

Another aim was to develop the used assay technologies utilizing upconversion to reach extreme sensitivities. Reagents and conditions in analog microtiter plate assay for cTnI were thoroughly investigated to fine-tune the performance, and the limit of detection (LoD) reached an unprecedented low value of 0.13 ng/L for an analog assay. In addition, a mechanical actuator for automation of a lateral flow assay for cTnI was fabricated via 3D-printing, and when combined with the improved UCNPs, an LoD of 1.5 ng/L was reached, bringing high-sensitivity point-of-care detection of cTnI a step closer to reality.

KEYWORDS: cardiac biomarker, luminescence, nanoparticle monodispersity

TURUN YLIOPISTO
Teknillinen tiedekunta
Bioteknologian laitos
Biotekniikka
Kirsti Raiko: Käänteisvirittеiset nanopartikkelit sydänperäisen troponiini I:n äärimmäisen herkässä havaitsemisessa
Väitöskirja, 133 s.
Tekniikan tohtoriohjelma
Syyskuu 2023

TIIVISTELMÄ

Herkkien immunomääritysmenetelmien kehitys on jatkuvan kiinnostuksen aiheena diagnostiikan tutkimuksessa. Herkät biomerkkiainetestit ovat haluttuja etenkin sydänkohtauksen kaltaisissa tiloissa, jossa merkkiaineen pitoisuus verenkierrossa kasvaa samalla, kun hoitoennuste heikkenee. Yksi merkittävimmistä immunomääritysten herkkyyteen vaikuttavista tekijöistä on määritysleima, joka sitoutuu analyyttiin ja tuottaa mitattavan signaalin. Käänteisvirittеisten nanopartikkelien (engl. *upconverting nanoparticles*, UCNP) kyky muuntaa matalaenergistä viritysvaloa korkeaenergiseksi emissioksi tekee niistä lupaavan määritysleiman herkkiin immunomäärityksiin, koska UCNP:iden signaalin mittaus voidaan tehdä niin, ettei autofluoresenssista koituvaa taustasignaalia havaita, mahdollistaen äärimmäisen herkät immunomääritykset. UCNP:iden taipumus sitoutua epäspesifisesti erilaisiin pintoihin ja muodostaa erikokoisia kasaumia on hidastanut niiden käyttöönottoa herkkinä immunomääritysleimoina. Tämän ominaisuuden on osoitettu riippuvan voimakkaasti partikkelien pintakemiasta.

Tämän tutkimuksen tavoite oli tutkia UCNP:iden pintakemiaa ja hyödyntää niitä määritysleimoina erilaisissa cTnI:tä havaitsevissa immunomäärityksissä. Tutkimuksessa selvitettiin UCNP:iden poly(akryylihappo) (PAA) -pinnoituksen onnistumiseen vaikuttavia tekijöitä ja onnistuttiin merkittävästi vähentämään PAA-pintaisten UCNPeiden epäspesifistä sitoutumista ja kasautumistaipumusta. Näitä UCNP-leimoja verrattiin muulla tavoin pinnoitettuihin UCNP-leimoihin mikrotiitterilevypohjaisessa immunomäärityksessä käyttäen joko analogista tai digitaalista mittausmenetelmää, sekä lateraalivirtausmäärityksessä.

Toinen tavoite oli kehittää käytettyjä määritysmenetelmiä äärimmäisten herkkyyksien saavuttamiseksi. Mikrotiitterilevymäärityksen reagenssit ja toteutusmenetelmä tutkittiin tarkoin ja hienosäädettiin. Tällä tekniikalla saavutettiin 0,13 ng/L havaitsemisherkkyys cTnI:lle, mikä on ennätyksellistä analogisissa mikrotiitterilevymäärityksissä. Lisäksi suunniteltiin mekaaninen 3D-tulostettu laite automatisoimaan cTnI:tä havaitseva lateraalivirtausmääritys. Yhdistettynä paranneltuihin PAA-UCNP:ihin, saavutettiin 1,5 ng/L havaitsemisherkkyys, mikä tuo äärimmäisen herkät cTnI:n vieritestausmenetelmät askeleen lähemmäs todellisuutta.

ASIASANAT: sydänmerkkiaine, luminesenssi, nanopartikkelien yksittäisyys

Table of Contents

Abbreviations

ASSURED	affordable, sensitive, specific, user-friendly, rapid and robust, equipment-free, and delivered
CLSI	Clinical & Laboratory Standards institute
cTnI and -T	cardiac troponin I and T
DBU	organic base 1,8-diazabicyclo(5.4.0)undec-7-ene
DLS	dynamic light scattering
EDC	1-ethyl-3-(3-dimethylaminopropyl)carbodiimide
ESA	excited state absorption
ETU	energy transfer upconversion
GSA	ground state absorption
hs	high-sensitivity (assay)
IUPAC	International Union of Pure and Applied Chemistry
LFA	lateral flow assay
LoD	limit of detection
Mab-PAA-UCNPs	monoclonal antibody-functionalized PAA-coated UCNPs
MPA	microtiter plate assay
sulfo-NHS	N-hydroxysulfosuccinimide
OA	oleic acid
PAA	poly(acrylic acid)
PAA(DBU)-UCNPs	poly(acrylic acid) coated UCNPs, coated by using DBU as pH adjusting agent in PAA-coating phase
PAA(NaOH)-UCNPs	poly(acrylic acid) coated UCNPs, coated by using NaOH as pH adjusting agent in PAA-coating phase
POC	Point-of-care
SA	streptavidin
SA-PEG-UCNPs	streptavidin functionalized polyethylene glycol coated upconverting nanoparticles
StDev	standard deviation
TEM	transmission electron microscope
T-line	test-line
UCL	upconversion luminescence
UCNP	upconverting nanoparticle
URL	upper reference limit

List of Original Publications

This dissertation is based on the following original publications, which are referred to in the text by their Roman numerals:

I Brandmeier J.C., Raiko K., Farka Z., Peltomaa R., Mickert M.J., Hlaváček A., Skládal P., Soukka T., Gorris H.H. Effect of Particle Size and Surface Chemistry of Photon-Upconversion Nanoparticles on Analog and Digital Immunoassays for Cardiac Troponin. *Adv Healthc Mater*. 2021;**10**:2100506.

II Raiko K., Lyytikäinen A., Ekman M., Nokelainen A., Lahtinen S., Soukka T. Supersensitive photon upconversion based immunoassay for detection of cardiac troponin I in human plasma. *Clin Chim Acta*. 2021;**523**:380-385.

III Raiko K., Nääjärvi O., Ekman M., Koskela S., Soukka T., Martiskainen I., Salminen T. Improved sensitivity and automation of multi-step upconversion lateral flow immunoassay using 3D-printed actuation mechanism driven by kitchen timer. Manuscript.

1 Introduction

Heterogeneous sandwich immunoassays are a cornerstone of biomedical diagnostics. They involve capture antibodies immobilized on a surface, on which the patient sample and reporter-conjugated antibodies are added, either in one or two steps, with washes in between. The assayed biomarker is bound by the capture antibody and the reporter-conjugated antibody labels the target via a second epitope. The reporter signal is thus proportional to the quantity of biomarker on the surface. The antibodies used, surface and method for immobilization, method of separation, reporter and the readout mode together mostly determine the sensitivity of the assay technology. [1]

Upconverting nanoparticles (UCNPs) are inorganic lanthanide crystals doped with trivalent lanthanide ions. Due to long-lived ladder-like metastable energy states of the lanthanides, they are capable of piling the energy of several photons and releasing it as a higher energy light quantum, leading to conversion of lower energy light to higher energy excitation.[2] Due to this process, which does not occur in any other material, can be used to spectrally eliminate autofluorescence originating from plastics and biological materials present in immunoassays. Background-free detection theoretically enables extreme sensitivities in assays, which is why UCNPs are considered as highly promising immunoassay reporters. [3] Time-resolved fluorescence measurement is a widely applied approach in autofluorescence elimination, however, it requires more sophisticated and expensive hardware compared to measurement of UCNPs.[4,5]

A major factor hindering the usage of UCNPs as assay reporters has been their tendency to non-specifically bind to solid surfaces in assays and to each other forming clusters, leading to uncertainties in measurement results.[6] Surface chemistry of UCNPs determines their interactions with their surroundings, and it has been established that by studying and modifying the surface chemistry, these unwanted tendencies can be reduced.[7–10] Improving the surface chemistry of UCNPs has been of major interest in upconversion assay development. Despite difficulties, several different UCNP-utilizing assays have been developed and they have gained momentum among biomedical researchers. In a cavalcade of

publications, UCNPs have been shown useful in sensitivity improvement in many different assay technologies. [11–15]

Cardiac events are usually diagnosed via detection of cardiac troponin proteins,[16] which partake in the muscle contraction of the heart.[17] In cardiac damage, troponins are released into the bloodstream, and their concentration rises with time after the damage has taken place.[18] The prognosis of cardiac patients depends heavily on how early the damage is diagnosed. With more sensitive immunoassays the elevated troponin values can be detected earlier, improving patient outcomes.[19] Current high-sensitivity troponin assays aim for limit of detection below the level encountered in the bloodstream of healthy patients.

2 Literature review

2.1 Immunoassays

2.1.1 Fundamentals of heterogeneous assays

An immunoassay is a method for detection and most often quantification of biomolecules or other biological species in a liquid sample. The technology is based on the ability of antibodies to specifically detect and bind a determined target (analyte). Various formats exploiting this theory have been developed, but the most widely used system, the heterogeneous sandwich assay (Figure 1), involves immobilized capture antibodies on a solid surface, referred to as the solid phase (as opposed to a homogeneous assay, where no solid phase is involved). The capture antibodies bind a specific molecular recognition site on the analyte (epitope), via the corresponding paratope on the antibody. The next step is addition and binding of a detection antibody. There paratopes of capture and detection antibodies are usually specific to different epitopes, unless the analyte contains large amounts of the same epitope, for example when measuring bacteria or viruses. The resulting immunocomplex can be thought of as a sandwich of two antibodies and the analyte, hence the name of the method. In 1-step assays, the reporter and analyte are added simultaneously, instead of in two separate steps. After each addition and usually a subsequent incubation, unbound reagents are washed away in both 1- and 2-step assays. [20,21]

The detection antibody is coupled with a reporter, which is responsible for generation of a detectable and quantifiable signal, for example radioactivity, an enzyme catalysing a reaction detected via colour change, or direct emission of light. After formation of the immunocomplex, the signal of the reporter is detected. The intensity of the detected signal is proportional to the concentration of the analyte, and the analyte can be quantified based on a signal-response standard curve. [20,21]

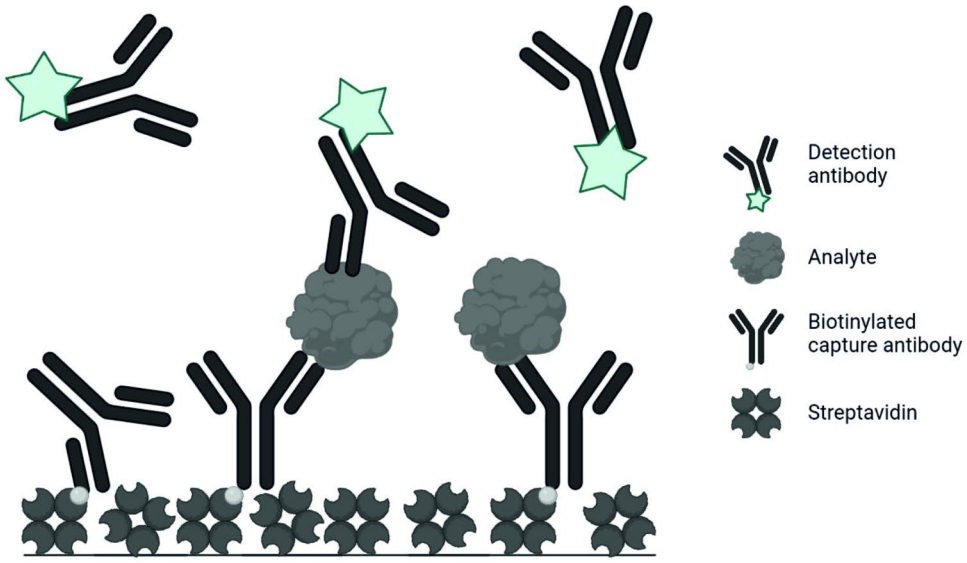

Figure 1. An example of a common heterogeneous 2-step sandwich immunoassay. Biotinylated capture-antibodies bind to streptavidin, which is immobilized to a solid surface. Analyte is captured from the sample by the capture antibodies, and all unbound components of the sample are washed away. Detection antibody, coupled to a reporter (green star), is added last, followed by washing of unbound reporter and measurement of signal of the remaining reporter. In 1-step assays reporter and analyte are added together. Figure created with Biorender.com.

Two main types of heterogenenous assays are non-competitive and competitive format. In the non-competitive format, the measured reporter signal increases with the analyte concentration in the sample, as more analyte binds to the immobilized capture antibodies. However, the competitive format involves addition of an analyte analog, which competes for binding sites with the analyte in the sample. The detection antibody detects the bound analog instead of the analyte in the sample. Thus, the measured signal decreases with increasing concentration of analyte in the sample. The latter method is mostly used in case the analyte is too small for sandwich formation around it. [1] In this thesis, the discussed assays are all non-competitive, and thus competitive assays will not be discussed further in this section.

2.1.2 Assay performance evaluation

Sensitivity of an assay is mostly considered as the key performance characteristic describing the usability of an assay, as it refers to lowest concentration of an analyte reliably distinguished from the background signal.[21] The key is to determine the concentration of the analyte that provides signal that is replicably higher than the signal of analyte-free sample. There are several standardized ways to empirically

determine and calculate analytical sensitivities, including Clinical & Laboratory Standards institute (CLSI) Guideline EP17-A2[22], or alternatively, International Union of Pure and Applied Chemistry (IUPAC) definition[23], and their choice depends on the specific situation. The CLSI guideline includes repetitive measurements of a large number of blank and low analyte concentration samples of different days for calculation of limit of detection (LoD), while IUPAC defines sensitivity as the slope of the standard curve. A third way, established by Ekins and co-workers,[21] incorporates the level of experimental error into sensitivity calculations. In their method, the LoD is defined as the analyte concentration on the standard curve corresponding to three times standard deviation of replicates of an analyte-free sample, added to the signal of the analyte free sample ($Signal_0 + 3xStDev_0$). This takes into account the instrumental background, measurement noise, and non-specific binding of reporter.[24–26]

Analytical specificity, on the other hand, refers to how well the assay can distinguish the target and other similar or non-similar constituents in the sample. It is heavily dependent on the cross-reactivity of the used antibodies, referring to their selectivity, i.e. how well the antibody distinguishes between the target analyte and other similar or non-similar substances.[1] However, low analytical specificity can also be caused by non-specific binding of the reporter itself, especially if the reporter is large in size.[6]

2.1.3 Antibody requirements

Perhaps the most significant factor in developing a functional immunoassay is the choice of the antibodies. Affinity and specificity of the antibody towards its target, and cross reactivity, are the main sensitivity affecting properties of antibodies in assays. Affinity of an antibody towards the respective analyte describes the strength with which they bind, and can be quantified as a special case of equilibrium constant. Affinity constant K_A is calculated as the ratio of concentration of antibody-analyte complex, to product of concentrations of analyte and antibody separately (equation 1). This can also be calculated via rate constants as the ratio of rate of binding reaction divided by rate of dissociation of analyte from antibody (k_{on}/k_{off}). [1,27,28]

$$K_A = \frac{[antibody+analyte]}{[antibody]\ x\ [analyte]} = \frac{k_{on}}{k_{off}} \quad (1)$$

The stronger the affinity of the antibody is towards the analyte, the faster, or more permanent, the formation of immunocomplex is.

The total binding strength of an antibody is not only dependent on the affinity of a single binding site to the target, but is also affected by an avidity, or multivalency,

effect. Avidity is a combined strength of more than one binding site interacting with a target molecule. Multivalent binders may bind a multivalent analyte via more than one epitope at once. Thus if one binding site dissociates, other paratopes may keep the binder in place until re-binding, instead of the binder diffusing far from the analyte. Immunoglobulin G- type antibodies (the Y-shape depicted in Figure 1.) are bi-valent, and thus the total binding strength is dependent on the interaction of both binding sites with multivalent targets. In terms of the affinity constant, multivalency can shift the ratio more towards the bound form. [29,30] The avidity effect can also be exploited to improve sensitivity when using large reporters, usually nanoparticles, which can be conjugated with several antibodies on the surface of one reporter.[31,32]

2.1.4 Solid phase

Solid phase in an immunoassay refers to the surface on which the capture antibodies are immobilized, and thus, onto which the immunocomplex forms. Possible solid phases in heterogeneous sandwich assays include microparticles, plastic microtitration plates (microtitration plate assay, MPA, usually with 96 or 384 wells), or paper-like nitrocellulose (immunochromatographic assay, commonly known as lateral flow assay [LFA]).[33] The solid phase, on which the immunocomplex is immobilized, determines the entire assay format. MPAs are conducted on the bottom of a microwell, on which the immunocomplex is formed by adding and removing liquids containing the constituents of the complex in order. Microtiter plates can be manufactured from different materials with different optical properties, and the material should be chosen according to the application. [33] For example, when using luminescent reporters and reading total signal intensity in a well from above, it might be beneficial to use white wells to maximize light collection efficiency. However, the detection is based on enzymes producing a coloured product from a substrate, transparent wells should be used for colorimetric detection. Such a plate would not be suitable for sensitive detection in measurement of light-producing reporters, as light can be lost through the transparent walls. Transparency of the well bottom is mostly dependent on the measurement hardware.

LFAs are, on their simplest, conducted on narrow strips of porous material, in which reagents flow by capillary action, but often they are composed of a mix of a few different materials with different roles (Figure 2). The first parts on the strip are sample pad and a conjugate pad. Their names are descriptive of the roles, as the sample to be analysed is deposited on the sample pad. Sample pad can also have integrated functions besides absorbing the sample, such as filtration of sample matrix components to decrease intereference.[34] The sample then flows to the conjugate pad, hydrating and dissolving the dried reporter conjugates. Conjugate pad is often fabricated using highly absorbent but inert glass fibre. The reporter-conjugate and

sample containing solution then flows on the following part, the nitrocellulose membrane, also known as the analytical membrane. The membrane contains the capture antibody immobilized as a narrow test line within the pores, followed by a control line. The last part is the absorbent pad, which functions as the engine and waste chamber of the assay. The capacity of the absorbent pad should be sufficient to absorb the volume of all liquids used in the assay and maintain the flow throughout the duration of the assay before reporter readout. [35]

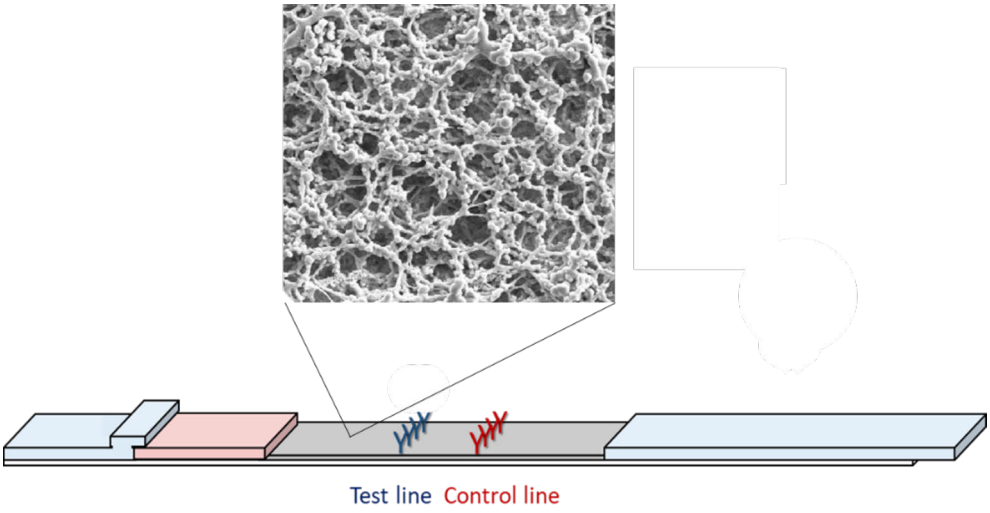

Figure 2. Example of a lateral flow assay strip. The first (from left to right) pad (blue) is the sample pad, the second one (red) the conjugate pad where reporter-conjugated antibodies can be dried, the third material (grey) is nitrocellulose, where the capture antibodies are immobilized. Last (largest) pad is the absorbent pad, functioning as the engine of the assay, maintaining capillary flow throughout the assay. Scanning electron microscopy image of a type of nitrocellulose modified from Cytiva [36], shows the highly porous structure of nitrocellulose, enabling a vast surface area for reagent binding

An advantage of LFA over MPA, brought upon by its structure, is the possibility of using a third antibody to form a control line. Aim of the control line antibody is to bind only the reporter, and is usually an anti-species antibody for the species where reporter antibodies are derived from. Signal from the control line informs the reader that reporter has flown past the test line. If no signal is detected on the control line, possible absence of signal from the test line may not be due to lack of analyte, but also due to lack of flowing reporter.[35]

LFAs are usually aimed at point-of-care (POC) applications, as opposed to MPAs, which are generally conducted in central laboratories. POC assays are, as the name implies, aimed to be used near the patient, and usually designed as simple and rapid tests for quick results.[37] The most commonly known examples are the home

pregnancy tests and Sars-COV-2 home tests. POC assays are expected to comply with ASSURED criteria, defined by the World Health Organization: affordable, sensitive, specific, user-friendly, rapid and robust, equipment-free, and delivered (accessible to end users).[38]

A high variety of different nitrocellulose types has been developed. They vary, among other factors, by surfactant quantities, protein absorption capacities, and most important of all; average pore size, main determinant of the flow rate. [39] Flow rate is the key factor limiting the choice of antibodies in the assay. The larger the pore size, the faster the flow, leaving less time for the immunocomplex to form on the test line. The opposite is true for smaller pore sizes.[39,40] For the most sensitive assays, slower membranes are often desired, however this compromises the rapidity aspect mentioned in the ASSURED criteria. On the other hand, using a faster membrane may compromise the sensitivity, although it can be optimized by developing antibodies with as high affinities as possible, or utilizing extremely high affinity interaction properties of biotin and streptavidin[41]. [40,42]

All solid phases have characteristic functional groups which can interact with the reporter, causing non-specific binding, which increases background in detection. This is why blocking is an essential step in heterogeneous assays. Plastic surfaces are often blocked with non-functional proteins, prioritizing high availability and low cost, such as bovine serum albumin[43]. The same approach can be used in blocking some or all materials used in LFAs.[39] Other possible blockers may depend on other components of the assay. For example, if a reporter is a polymer-coated nanoparticle, one may want to add a shorter version of the coated polymer to the blocking solution, to block all sites where the polymer could attach to, reducing the probability of the reporter itself non-specifically attaching to the surfaces.[44]

2.1.5 Immobilization

The solid phase also affects the method of immobilization. Immobilization of capture antibodies to solid phase can be done via passive coating directly. In direct passive coating of capture antibodies to 2D-surfaces, the orientation of the antibodies cannot be controlled and thus a portion of them will bind in a manner which leaves the paratopes inaccessible.[45] In addition, the binding event may alter the conformation of the protein, undermining the affinity towards the analyte.[33,46,47] As an alternative, the immobilization of capture antibodies can be mediated by using a separate binder such as a protein or a peptide, among other approaches.[48] A popular approach is to passively coat streptavidin (SA) to the surface while using biotinylated antibodies.[49–52]

When using SA to facilitate immobilization instead of direct passive adsorption of antibodies, it is possible to site-specifically biotinylate antibodies, to ensure

minimum biotinylation on the detection sites. This can be done by choosing a coupling chemistry targeting specific moieties on the antibody.[53] Such an approach leaves a maximum amount of antibodies reactive, and thus able to participate in analyte detection. SA as a protein may also undergo a change in conformation upon adsorption to the surface[54,55], however, it is more likely that one of the four binding sites remains active, compared to the two binding sites on one end of an antibody. It also depends on the properties of the antibody, how well it is adsorbed to plastic surfaces, and thus using SA as an intermediate coating, any type of biotinylated antibody can be easily used as a capture without the need to develop novel coating methods.[56]

The passive coating of antibodies directly is more commonly used in lateral flow assays, where the solid phase matrix is more 3D than 2D, and so the antibodies bind to the pores of the material and the liquid reagents flow through the pores.[42] As the nitrocellulose matrix is highly porous, the surface area for binding is immense compared to a standard 96-well plate bottom, thus being able to house massive amounts of antibodies in a relatively small volume[57–59], decreasing the significance of some antibodies binding in an unfavourable position. Note, thus, that the illustration in Figure 2 is not factual regarding the positions of antibodies on the nitrocellulose, as in reality the antibodies are scattered in all possible directions throughout the depth of the membrane.[59]

2.1.6 Separation on microplate

Heterogeneous sandwich assays can be designed as 1- or 2-step assays, differentiated by the number of separation steps involved in the assay procedure. In 1-step assays, reporter and analyte are added on the immobilized capture antibody together before unbound reporter and sample material are washed away. Separation, usually conducted as a washing step in heterogeneous immunoassays, aims to remove unbound analyte and reporter, but also to decrease interference due to matrix effects in 2-step assays. Matrix effects are a diverse group of non-specific binding mechanisms brought upon by proteins and components in the sample material, such as serum or plasma.[60–64] These may result in false negatives through masking of epitopes via for example autoantibodies[65,66], or paratopes if the assay antibodies lack sufficient specificity[60–64], or false positives through non-specific binding of the reporter to solid surface mediated by a matrix component[67].

In 1-step assays the entire sandwich is formed in the presence of the sample material, leaving the immunocomplex formation exposed to all the possible sources of interference from the matrix. [60–64] In 2-step assays, the analyte is incubated with the capture surface first, followed by a separation (i.e. washing) step before addition, incubation and washing of unbound reporter. This is why 2-step assays are often

preferred, as the analyte is captured by the capture antibodies from the sample material, followed by washing to remove as much of the interference causing agents of the sample material as possible, before addition of the reporter.[62,63] Although it is unlikely that all interference causing agents can be washed away, 2-step assays can theoretically be more sensitive.

Wash buffer composition can be designed according to the step, and thus it can vary between washing steps in the assay depending on what is aimed to be removed. Failure to wash efficiently may lead to high background signal due to either the remaining non-specific binding causing agents originating from the sample material after sample incubation, or reporters bound non-specifically to the solid surface after reporter incubation. On the other hand, an excessively exhaustive washing step may lead to loss of analyte-specific signal due to mechanical or chemical removal of any crucial reagent from the surface, or chemically interfering with the immunodetection reaction between epitopes and paratopes. [68]

In general, separation phases in MPA are simple and easy to modify according to needs, in terms of number of wash cycles and the desired buffer optimized for each washing step. Washing is often done using a separate plate washer, a standard piece of equipment in all immunoassay labs today. In centralized laboratories, all such steps are automated.

2.1.7 Separation in lateral flow

Separation in LFA is more complex to modify according to needs compared to MPA. On one hand, LFA is possible to conduct entirely by addition of just the sample with no separation buffers if the sample matrix is appropriate and the reporter has been dried on the test strip. In a standard home pregnancy test, for example, urine provides the analyte as well as the washing solution. On the other hand, if the sample matrix is more viscous or the volume is insufficient, wash buffers need to be applied to remove as much of the unbound reporter as possible. The reporter left along the nitrocellulose will increase background making it more difficult to distinguish a faint test line from the surrounding membrane, being detrimental to the sensitivity of the assay.[35,42]

The need and ability to integrate washing steps are limited, among others, by the flow rate, also known as the capillary flow time or wicking time, of the nitrocellulose membrane. The flow rate is proportional to the average pore size. The larger the pores, the faster the flow, and thus faster theoretical time to achieve measurable signal from the test line, as the reagents flow faster. However, slower flowing membranes enable theoretically improved sensitivity especially for slow kinetics immunoreactions, as the slower the flow, the more time is available for the immunoreagents to react and the complex to form. In general, the desired flow rate

of nitrocellulose is a compromise between number of different steps in the assay in a reasonable assay time, versus intensity of test line. [39,40,43]

Faster flow rate nitrocellulose enables faster wash steps, but decreases sensitivity because the immunocomplex will have less time to form on the test line, while slower nitrocellulose enables use of lower affinity antibodies (widening the number of possible analytes detected) but decreases possibilities for many steps in the assay procedure.[43]

To fulfil all ASSURED criteria, especially the combination of user-friendliness, freedom of equipment, and sensitivity, using an LFA-platform, has led to development of a wide array of flow control approaches to enable automation of multi-step POC-LFAs. Because antibodies can only be improved so much, increasing complexity of assay procedure towards resembling that of an MPA, is one of the few tools in improving sensitivity. To reduce background noise, a washing step chronologically after immunocomplex formation is desired, but manual addition of the wash buffer compromises the ASSURED criteria. Also, increasing the interaction time for immunocomplex formation improves sensitivity of detection. Thus, passive methods to induce multi-step LF assays have been developed. They include creating flow paths of different lengths to achieve sequential flow fronts to the test line at different time points, by either appropriate cutting of materials[69,70] or wax printing of labyrinths[71–73]. Slowing down of flow in different paths via passive flow control techniques such as wax pillars[74] or dissolving wax barriers[75,76], dissolving barriers[77,78], or using sugar to increase viscosity[79], using overlapping materials of different porosities and thus flow rates[80,81]. Different valves and switches have also been developed be applying the mentioned flow control methods. In addition to timed washing steps, these can also be used in sensitivity enhancement by slowing down the flow of sample and reporter before reaching test line, to create a type of pre-incubation step for the first half of the immunocomplex. [77,82,83] Centrifugation has also been used as a flow control method in paper-based diagnostics.[84,85]

2.1.8 Reporter systems

Alongside antibodies, another sensitivity-determining factor is the reporter system.[86–88] A theoretical optimal reporter should be small in size to prevent steric hindrance in detection and diffusion, thus improving reaction kinetics compared to larger ones. However, increasing the size of the reporter may also bring upon advantages. When using large reporters, it may be possible to conjugate more than one antibody to the surface, improving the sensitivity through avidity effect.[32] The reporter should also have an infinitely high specific activity, referring to the number of detectable events, or “counts”, per unit time per unit weight of labelled material.[89]

Such reporter enables maximum steepness of analyte-signal response curve within a minimal acquisition time. The reporter should also enable a reliable, repeatable and quantifiable increase in measured signal with increase of analyte. In other words, linear increase of analyte concentration should produce a linear response, requiring the reporters to be equal in specific activity to each other.[21] This requirement may be undermined by clustering of many reporters to form an aggregate which still recognizes only one analyte. Lastly, the reporter should be easily conjugatable to antibodies.

First immunoassays utilized radioisotopes,[90] which were easy to conjugate to antibodies and their small size enabled minimal steric hindrance to detection and diffusion rates. However, to avoid damage to biomolecules, safety issues to laboratory workers, and impractical shelf-lives, only low activity isotopes were usable, but lead to long signal acquisition times.[26,91]

Next major improvement, which is also the gold standard used in immunoassays today, was the application of enzymes as reporters.[92] They are robust and enable signal enhancement, because one enzyme is capable of converting a virtually unlimited amount of substrate into a signal generating product.[93] Range of detection hardware was also increased, as substrate types could vary, including colorimetric, fluorescent and luminescent detection.[94] However, they are larger than radioisotopes, require a separate, meticulously timed, signal generation step. Also, as the enzymatic reactions mostly occur in solutions and the substrate scatters into the surrounding liquid, spatial resolution on the solid phase was not practically feasible.[26]

Introduction of directly fluorescent species such as quantum dots[95], fluorescent nanoparticles[86], or fluorescent chelates[96] as assay reporters helped overcome the issues with spatial resolution and addition of separate signal generation reagents, encountered with enzyme reporters. On the other hand, many fluorescent species are often subject to photobleaching, meaning that despite the reasonable specific activity, they withstand only a limited number of excitation-emission cycles before degenerating.[26,97]

Despite photobleaching, reporters differ also in other ways in stability. The shelf-life of radioimmunoassay reporters is only a few months due to their half-lives[91], and some reporters dissolve in aqueous environments without additives[98]. Despite sensitivity considerations when choosing a reporter, the stability-requirements of the finalized product should not be overlooked in assay development.

Conventional fluorophores exhibit a phenomenon called Stokes shift, meaning that the incident excitation light loses energy upon absorption to the fluorophore in non-radiative processes before being emitted.[99,100] Unfortunately, many other substances, such as biological materials, plastics[101], and other components unavoidably present in immunoassays also exhibit a similar property of luminescing upon excitation with light of sufficient energy, giving rise to autofluorescence. This

is detected as background noise in spectral measurements, reducing the maximum theoretical sensitivity of detection.[102,103] Lifetime of autofluorescence is relatively short-lived, dissipating within nanoseconds. This feature can be used to circumvent the issue of background noise with time-resolved fluorometry[4], based on using lanthanide ions with longer luminescence lifetimes, which are in the range ten to hundreds of microseconds.[104] By time-gating the spectral measurements to only measure the signal of long lifetime reporters after the autofluorescence has ceased, it is possible to exclude it from the measurements.[105]

In LFAs, the most important consideration when choosing a reporter is the intended use and end-user. Often, the simplicity of use is one of the highest priorities, in which case visually read reporters are of greatest interest, as they do not require a separate device for the readout. LFAs with visually read reporters are also more cost-efficient. The most used example, also utilized in standard commercial home-pregnancy tests, is a gold nanoparticle. When they cluster together on the test line in a sufficiently high concentration, they form a red-appearing line detectable by eye.[106]

Sometimes sensitivity is prioritized over affordability, in which case optical reporters can be employed.[88] Sensitivity enhancement of optically read compared to visual reporters in lateral flow applications has been established in various instances.[88,107–109] In addition to sensitivity enhancement, optical measurement enables quantitative analysis of POC-LFAs.[106] Several portable reader devices have been developed to enable POC applications of optically read LFAs. In the simplest form, any smartphone can function as one.[34,110,111]

2.1.9 Readout modes

In MPAs, optically detected reporters can be read in two different modes; analog and digital.[112] In analog mode MPAs, a total signal in wells is measured.[26,112] Lateral flow assays even with optical detection are always so far measured with analog detection.[34] Analog measurement for LFAs and MPAs are visualized in Figure 3a and b, respectively. Instrumental background and the blank calibrator signal (i.e. the non-specific binding) are both subtracted from the averaged signal of wells with the sample to be analysed, and the resulting signal intensity (specific signal) is used to indicate the concentration of the analyte in the well.[21]

If reporter is highly detectable and the specific, instrument background subtracted signal of blank calibrator is replicably close to zero, the instrumental background becomes the sensitivity limiting factor in analog measurements. As it was established in section 2.1.2, sensitivity is dependent on both the intensity and the variation of background subtracted signal of the blank calibrator. Thus, if the non-specific binding, i.e. the blank calibrator signal is close to zero, even small fluctuations in the instrumental background result to large relative variation in the

signal of blank calibrator. The analyte concentrations closest to zero can be masked by the variation originating solely from the instrument.[26,113]

However, digital assays are based on counting of single molecules, instead of measuring total luminescence of wells (visualized in Figure 3c). In digital two-step assays, the solid substrate with immobilized labelled immunocomplexes is imaged and the number of reporters is counted from the images, followed by similar calculations as in the analog measurement.[26,112] Theoretically, digital assays enable the most sensitive possible detection of analytes, as counting of single molecules can be considered to be the most accurate way to make a measurement.[114]. In digital detection, if the reporters are detectable enough to be distinguished from the image noise, the instrumental background can be neglected from the calculations, and thus the instrumental signal fluctuation will not affect the variation between replicates, as long as a threshold for signal intensity can be determined.[26]

In case of extremely low level of non-specific binding, the sensitivity limiting factor in digital assays can arise from a type of sampling error referred to as Poisson noise ($\sqrt{n}/n$, where n is the number of counted events).[115] Result of the equation gives the percentage error in digital analysis, which is equivalent to coefficient of variation percentage in analog measurements, an thus can be used to determine the reliability of digital measurements. If the non-specific binding corresponds to only a few tens of observed reporters, such as 30, the coefficient of variation originating from Poisson noise is 18%.

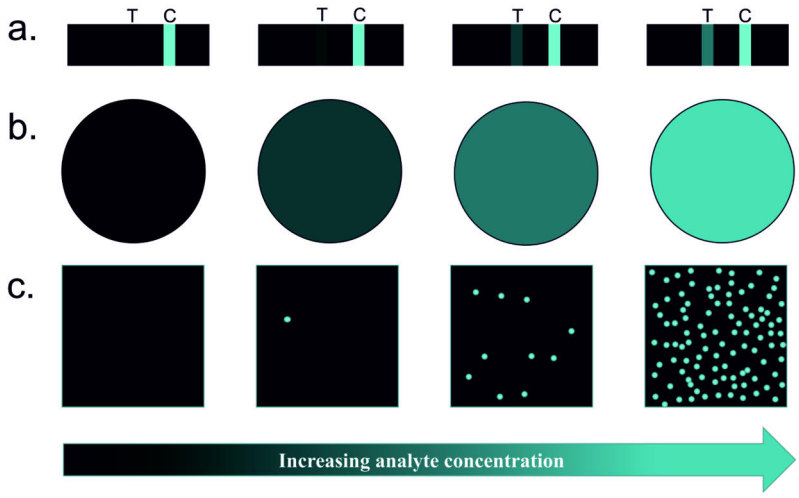

Figure 3. Visual representation of different readout-modes with a hypothetical serial dilution using the same optically read reporter in a sandwich assay. a) LFA with analog optical readout, signal strength of T (test)-line used to indicate reporter density, b) MPA with analog readout, where signal intensity from the well area is used to indicate reporter density and c) MPA with digital readout, where number of reporters is calculated from the solid surface. Figure adapted from Soukka and Gorris (2022).[26]

Some reporters may also exhibit differences in brightness. For example, in particle reporters, particles may aggregate and thus the signal measured for labelled analytes may differ based on the size of the aggregate, i.e. how many reporters have clustered together. This may lead to signal variation between replicates in analog measurements. In addition, non-specific binding of large aggregates to the solid substrate may significantly increase the background noise and its fluctuations in measurements, also leading to loss of sensitivity. However, in digital measurements, each spot of light can be counted as one event, or one analyte molecule, and thus the effect of brightness variation can be neglected, potentially leading to smaller variation between replicates. Also the effect of non-specifically bound aggregates is reduced to correspond to a count of 1, instead of a large signal burst. [26,87]

2.2 Upconverting nanoparticles

UCNPs are luminescent inorganic crystals doped with trivalent lanthanide ions, with diameter below 100 nm.[116] Interest in their application as immunoassay reporters has increased steadily throughout the millennium, and the reason lies in their luminescent properties. Unlike any material occurring in nature, UCNPs exhibit anti-Stokes luminescence, in which the wavelength of excitation light is wider than that of the emitted light, i.e. emitted light is of higher energy than the excitation light.[2,117]

The opposite direction of energy conversion in luminescence offers another alternative to elimination of autofluorescence as opposed to time-resolved measurements.[118] As energy conversion in autofluorescence is from high energy excitation light to lower energy emission, is it simple to design appropriate optical filters to filter out the noise while only recording upconverted light of shorter wavelengths. Removal of the requirement for meticulous time gating in data acquisition also leads to more affordable detection hardware. [119]

As per the law of energy conservation, emitting a higher energy light than the excitation light is not be possible without first absorbing the energy of two or more photons, stacking the energy, and subsequently emitting the energy in one light quantum. Certain lanthanides contain a large number of close energy levels, which form a photophysical ladder for cumulative energy absorption, which, together with the relatively long excitation lifetimes (metastable energy levels), make them the ideal component in UCNPs.[3]

Most prominent energy transitions involved in upconversion in UCNPs are excited state absorption (ESA) and energy transfer upconversion (ETU), illustrated in Figure 4.[2] In ESA, the ion is first excited from ground state to the first excited state, in a process called ground state absorption (GSA). Due to metastable energy states lasting even microseconds, it is possible for this process to be followed by

absorption of energy of another photon before relaxation, exciting the ion to the next energy state. [120]

ETU on the other hand, is a two-ion process, described by Francois Auzel in 1966. The ions involved are referred to as sensitizer and the activator, based on their roles in the process. The key requirement for the ion pair selection is that the difference between the metastable energy levels of the activator ion are sufficiently similar to the first excited state energy of the sensitizer.[121] The role of the sensitizer is to be excited by the excitation light and undergo GSA. While the host matrix provides sufficient proximity and spatial geometry, it is possible for the energy to be transferred from the sensitizer to the activator ion, leading to excitation of the activator, while the sensitizer relaxes as it donates the energy. [122] With powerful enough excitation light sources, it is possible for either the same, or another, sensitizer ion in proximity to undergo GSA and transfer the energy to the same activator before the lifetime of the second energy state of the activator is outlived.[122] This leads to stacking of the energy on top of the previous transferred photon.[3] Thus, it is possible for the emission from radiative relaxation from the activator to be of shorter wavelength than that of the excitation light, explaining the observed upconversion of light without violating the law of energy conservation.

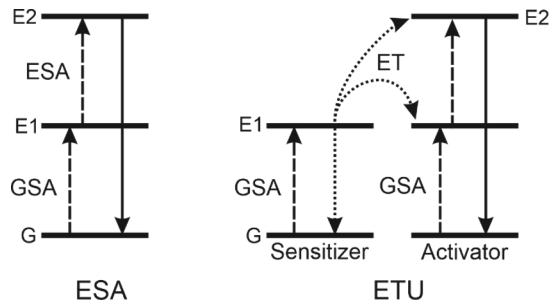

Figure 4. Most prominent energy transitions occurring in upconversion. In excited state absorption (ESA), the energy of two incident photons is absorbed subsequently, first allowing for ground state absorption (GSA) from ground-state to first energy level (E1) followed by ESA, lifting the ion to second energy level (E2). Energy transfer upconversion (ETU) is a two-ion process, where sensitizer undergoes GSA multiple times, donating the excitation energy to the activator ion.[123] Figure adapted from Auzel[123] and Nadort et al.[120]

Both processes require an excitation source with high enough power density. [124] Without sufficient quantity of photons per unit time being incident on the UCNP surface, the lifetime of the intermediate energy states is outlived and the ion relaxes, either via nonradiative or down-shifting routes. [125–127]

The ions are embedded in a host matrix to stabilize the dopant ions in sufficient proximity to each other. A host matrix must be optically transparent to both the

excitation and emission wavelengths. One of the most efficient structures for upconversion processes, and thus one of the most used structures in UCNPs, is composed of $NaYF_4$ doped with trivalent lanthanide ions, often ytterbium as the sensitizer and erbium or thulium as activators.[128],[120,128]

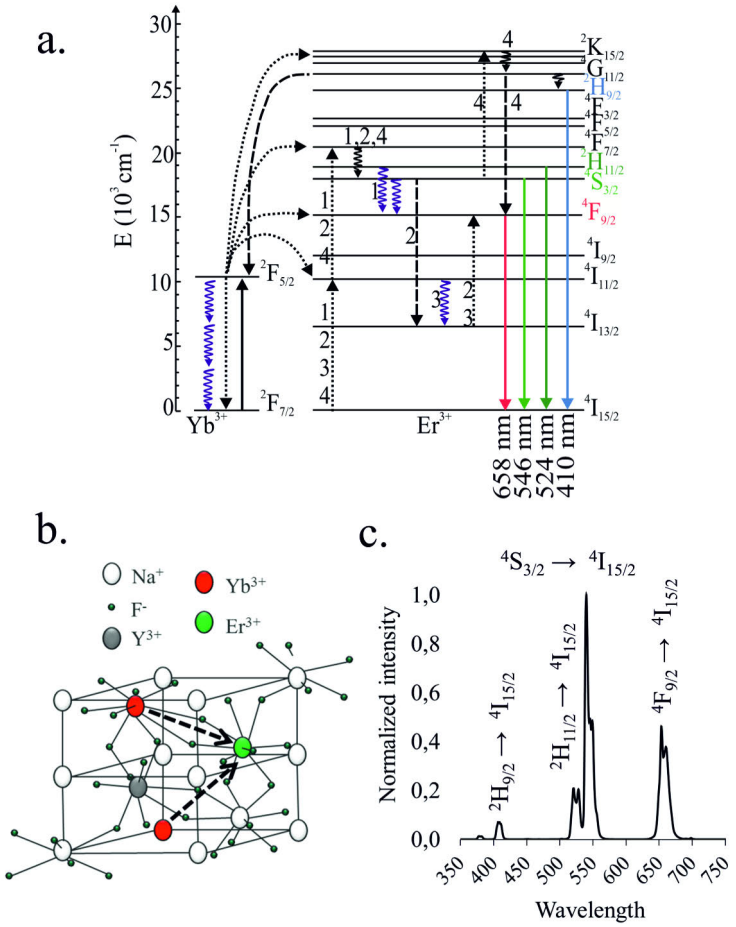

Figure 5. The relationship of **a)** energy transfer processes between sensitizer (Yb^{3+}, as example) and activator (Er^{3+}, as example), **b)** the structure and orientation of a cubic host matrix and the dopant ions (dashed arrows illustrate the energy transfer), and **c)** the measured upconversion emission spectra for oleic acid-coated $NaYF_4$ (17% Yb^{3+}, 3% Er^{3+}) - UCNPs in toluene, excited with 980 nm. The emission intensities are normalized with respect to intensity of emission maximum (540 nm for Er^{3+} -doped UCNPs). Many different paths can lead to origin of the red ~650 nm emission, and the arrows numbered 1-4 in **a.** show the four most suggested paths.[129–132] Figure a is adapted from Lahtinen (2019).[138] Figure b is modified from Wang, F. et al. (2010).[139]

The described ladder-like metastable energy levels and the energy transfer processes involved in Yb^{3+} and Er^{3+} doped UCNPs are visualized in the Jablonski diagram in Figure 5a. The direction of energy transfer between the ion pair and the orientation and structure of the host matrix is illustrated in 5b, and an example of emission spectrum measured from a specimen of such UCNPs in 5c. The upconversion mechanisms in the ETU process have been studied, but especially the mechanism for origin of the red emission band is under discussion. Figure 5a presents four of the most commonly discussed possible mechanisms.[129–132] However, as the red-green ratio has been observed to change depending on the environment the UCNPs are dispersed,[133–135] most likely they all occur, but the one taking place depends on the structure and current environment.[136,137]

Spectral properties and luminescence brightness depend on the identity and concentration of the dopant ions, power density of the excitation source, particle size, host matrix properties, and the environment such as temperature[140], but especially presence of water[141,142]. Different combinations of these properties alter the probability of different radiative and non-radiative (incl. quenching) energy transfer processes. There are many excellent reviews and research articles on how to avoid or exploit these effects in tuning the brightness, colour, and usability of the UCNPs in different applications, and the reader is advised to refer to those for more information on the topic.[3,120,124,140,142–144]

UCNPs fulfil most of the desirable properties for assay reporters discussed in section 2.1.3. Comparing to the first mentioned radioactive reporters, UCNPs have incredible specific activity which does not pose limitations to the detection[89], while also being non-radioactive so they are relatively safe to handle. Their readout requires no separate enhancement reagent addition step unlike some lanthanide chelate and enzyme-based systems, but are directly readable from the surface they are bound to, which also enables spatial resolution in multianalyte and digital detection applications. They are extremely photostable[145], withstanding a countless number of excitation-emission cycles, enabling archiving of assays and calibrating equipment with respect to UCNP brightness. Their inorganic nature makes them robust with practically infinite shelf-lives under optimal conditions. Combining the possibility for spectral elimination of autofluorescence to the immense specific activity makes UCNPs extremely detectable reporters which enable single molecule level detection in immunoassays.[146–148]

Their brightness, however, is a compromise with size.[149] The larger the UCNP the brighter is their specific activity. On the other hand, the larger the assay reporter the greater the steric hindrance in both diffusion in liquid samples in both wells in MPAs and porous materials in LFAs. In addition, large size leads to large surface area, making the reporter more susceptible to non-specific interactions with the solid phase.[6]

Presence of water is also an issue when using UCNPs. Aqueous environment not only quenches the upconversion luminescence,[133,135,150] but UCNPs with fluoride-based core structures will disintegrate to reach an equilibrium with respect to fluoride ions with the surrounding medium.[98,151–153] Thus, it is required to protect the integrity of the UCNPs by adding a sufficient concentration of free fluoride ions in the surrounding solution, or alternatively shield the particle with an appropriate coating.[152]

Despite being excellent assay reporters, their tendency to non-specifically bind to each other leading to cluster formation, and to solid phases leading to elevated background in measurements, has hindered harnessing their potential.[44,67] Cluster formation leads to differences in specific activity between reporter units binding to analytes, as the larger the cluster the brighter the signal measured for the specific analyte, leading to potentially non-linear increase of signal per increase of analyte concentration.[147,154,155] Particle aggregation has been noted as a fundamental problem in all nanoparticle utilizing applications.[156] These tendencies of UCNPs are specifically pronounced in biological fluids.[8,157] The main way to affect these properties is modification of the surface chemistry properties, as monodispersity, colloidality and hydrophilicity are highly charge-dependent.[9,10]

Most successful synthesis methods to yield UCNPs take place in organic solvents, yielding particles that are not dispersible in water, usually having a non-polar ligand coating,[158][159] although research is still being conducted on developing ligand-free synthesis methods to yield UCNPs dispersible directly to both polar- and non-polar solvents.[160] Immunoassays, on the other hand, always involve aqueous buffers and samples, which is why surface chemistry of UCNPs has to be the first consideration when beginning to use UCNPs as assay reporters. In addition to water solubility, the surface chemistry approach should yield highly monodisperse particles, which are also bioconjugatable, but inert enough to not promote non-specific binding to substrate surface or each other.

2.3 Surface chemistry of upconverting nanoparticles

A wide array of different approaches have been developed to render hydrophobic, most often oleic acid (OA)-coated UCNPs hydrophilic, each with their own strengths and weaknesses. They can be divided into categories based on whether OA is preserved on the surface or removed, and whether the removal is done by washing, or 1- or 2-step exchange processes.[9,159] When a hydrophobic ligand is removed from the surface and the UCNP is bare in solution, it is inherently dispersible in aqueous solutions.[152,161] However, addition of a suitable surface ligand is necessary to facilitate conjugation to desired biodetection molecules. For this purpose, the ligand

should have functional groups such as COOH, NH_2, sulfonate, thiol or maleimide.[10,162] Some of the different approaches have been outlined in Figure 6.

Surface chemistry approaches not involving removal of OA include modification of OA from hydrophobic to hydrophilic via oxidation of the carbon-carbon double bonds in the fatty acid chain.[163–165] Another way is to utilize the hydrophobicity in coating, using an amphiphilic ligand.[159,166,167] In this case, a bilayer forms around the particle, with the hydrophobic tail of the amphiphile intercalating in between the OA tails, leaving hydrophilic heads interacting with the surface.[9] A third way to approach the topic is to encapsulate the entire OA-capped UCNP within a shell. This can be done using comb-shaped amphiphilic molecules, which form a mosaic shell around the particle.[168] The pieces of mosaic can later be covalently attached to each other, forming a uniform shell.[169–171] A more widely utilized shell material is silica and the coating is done in a reverse microemulsion process of silicon alkoxide, UCNPs surfactants, and ammonia.[172] Encapsulation processes may lead to aggregation during coating, as more than one UCNP may be encapsulated together, leading to a wide size distribution.[9]

In ligand exchange approaches, the desired coating ligand should have functional groups which can coordinate to the surface with higher affinity than OA.[173] Coordinating groups able to interact with the positively charged lanthanide ions include -SH, $-NH_2$, -COOH, and $-PO_3H$.[10] Different groups have different coordinating affinities, and also avidity effect can be utilized, meaning that a polymer with a large number of coordinating groups attaches to the nanoparticle surface with greater strength compared to ligands with just one or few groups.[173] When coating with negatively charged polymers, coating density is a highly determining factor in monodispersity and colloidality. Uneven covering of negative polymer on positively charged UCNP surface may lead to aggregation and precipitation of UCNPs in aqueous solutions.[174] Thus, the usability of the final coated particle is more dependent the coating procedure than the ligand itself, although both are crucial factors.

One step ligand exchange from OA to a polar ligand has been shown by Naccache and others with citrate for $NaGdF_4$-UCNPs.[175] According to the group, the yielding UCNPs were dispersible in aqueous solutions with long-lived colloidal stability. However, it has been noted that if citrate-coated UCNPs are not coated further, they aggregate upon removal from buffer containing a sufficient amount of free citrate.[176,177]

Two-step ligand exchange is becoming the most popular method of rendering UCNPs hydrophilic and subsequently coating them with the desired ligands, as the protocol for OA-stripping is not dependent on the final ligand for coating. Simplest way is to remove OA using low pH solutions (acid washing) yielding bare UCNPs, which are as themselves water dispersible in low pH.[161,178] OA protonates when pH

is reduced below 4, leading to detaching from the surface.[161] This approach is not the most successful one in yielding monodisperse UCNPs, and later on it has been discussed, supported by empirical data, that the acid washed bare UCNPs tend to minimize their surface energy by default by forming aggregates.[157,174,179,180] This leads to UCNPs in clusters of wide size distribution even after addition of a ligand in the second step of the ligand exchange.

The most successful two-step ligand exchange method utilizes nitrosyl tetrafluoroborate ($NOBF_4$) in the presence of the amphiphilic solvent dimethylformamide (DMF) and non-polar cyclohexane phase. The process is also based on pH change. Although DMF is usually anhydrous, the reagent still contains approximately 0.2% residual water, capable of reacting with $NOBF_4$, yielding an acidic environment through formation of nitrous acid, following the equation 2.[181]

$$NO^+ + H_2O \rightleftharpoons HNO_2 + H^+ \quad (2)$$

As OA is removed from the surface, UCNPs are stabilized by the BF_4^- ions weakly coordinating to the lanthanides on the surface, migrating to DMF, leaving OA in the non-polar phase. On the other hand, the intermediate phase is not highly stable, and even slight differences in protocols can significantly affect the quality of resulting UCNPs.[159] Comparing a two-step ligand exchange strategy using BF_4^- as an intermediate to acid wash in coating with polymers, it has been noted that the two-step method yields significantly more monodisperse UCNPs in aqueous solutions.[157,182] The second step of the ligand exchange depends on the ligand itself, or more specifically, the group of the ligands via which it is aimed to coordinate to the lanthanides on the UCNP surface.

A wide array of different ligands have been tested in two-step ligand exchange to induce hydrophilicity and monodispersity in aqueous solutions and biological fluids, as well as facilitate conjugation to biodetection molecules. In a study by Nsubuga et al (2018), UCNPs were coated with O-phospho-L-threonine, polyethylene glycol -phosphate and alendronate ligands, using the two-step ligand exchange with BF_4^- intermediate. As a result, all ligands produced a colloidally stable monodisperse solution of UCNPs.[7] An example of a widely used ligand coordinating through -COOH groups poly(acrylic acid) (PAA). It is a negatively charged polymer of acrylic acid, where each monomer has a -COOH group for coordination, leading to efficient coating via avidity effect. In addition it is branched, leaving a large number of -COOH groups still available for bioconjugation.[174]

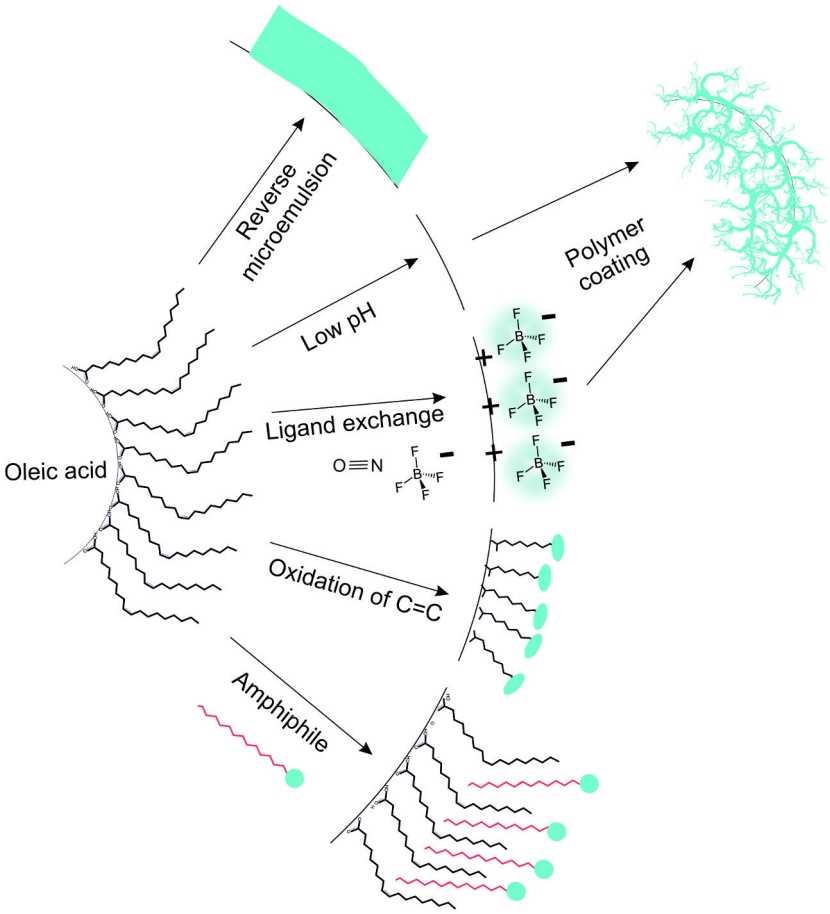

Figure 6. Summary of different surface chemistry modification approaches to yield hydrophilic UCNPs from hydrophobic OA-capped UCNPs. From top down: Reverse microemulsion method to directly coat the OA surface with solid silica. Low pH to remove OA from the surface to yield bare UCNPs, or ligand exchange to replace the OA with BF_4^- ions, before addition of surface coordinating polymer, such as PAA. Oxidation of carbon-carbon double bond with a hydrophilic capping group to modify the OA itself. Addition of an amphiphile to intercalate with the hydrophobic hydrocarbon tails, leaving the hydrophilic group interacting with the environment.

Significance of coating protocol to monodispersity and quality of the UCNPs has been demonstrated using PAA-coated UCNPs, results supporting the superiority of two-step ligand exchange mediated by BF_4^-- intermediate compared to acid washing and subsequent coating. [157,174] In a study comparing an array of small molecules and polymers as surface ligands on UCNPs coated with two-step ligand exchange, it was noted that polymers like PAA lead to a high surface coverage compared to small molecules. In addition to being tightly wrapped around the particle through -COOH

groups, PAA-coating yields highly colloidally stable UCNPs due to an abundance of charged -COOH groups still left to interact with the aqueous environment.[174]

Making a comprehensive comparison between different ligands is highly challenging, as it is difficult to devise a protocol, which would lead to entirely comparable results between different ligands, as it depends on the nature of the ligand which coating conditions are optimal. For example, when PAA is used as a ligand, it is beneficial to increase the alkalinity of coating reaction above pH 9 to deprotonate the carboxyl groups, facilitating coordination to positively charged lanthanide ions on the UCNP surface. However, when the interaction between the UCNP and ligand is different, the optimal coating conditions change. Thus, the optimal ligand and optimal coating process should be found for each intended use and many options may be possible.

2.4 Upconversion assay technologies

2.4.1 Non-specific binding

Non-specific binding of UCNPs to solid substrates has been a major hindering factor in developing ultrasensitive upconversion immunoassays. Although the level of non-specific binding is not necessarily higher with UCNPs compared to other reporters, the extreme detectability of the reporter produces an immense contrast over the instrument background.[183,184] Mechanisms for non-specific binding of UCNPs in microtiter plate based immunoassays has generally been understood to be dependent on a combination of matrix effects of biological media, and surface chemistry of the UCNPs.

Matrix effects refer to non-specific binding of UCNPs to each other or solid substrates mediated by proteins or components in the samples which adsorb to the well surface, and interact with the reporter. A study of Kuusinen et al. (2022) focused on enriching fractions of blood plasma, which lead to the highest non-specific binding in assays utilizing PAA-coated UCNPs, to trace the factors most responsible for the effect. They concluded that positively charged complement component C1q had a significant role in mediating the high background signals, and that the mechanism was most likely charge related. Also, addition of heparin and NaCl in appropriate quantities improved the signal-to-background ratio in assays.[67] Another study by Liang et al. (2022) studied the adsorption of serum proteins to PAA and PEI-coated UCNPs, and concluded that the protein corona on PAA-coated particles was thinner, in other words, PAA-coating was less prone to protein adsorption. This supports the choice of PAA as an appropriate immunoassay reporter coating, as smaller tendency to interact with proteins will reduce the probability of non-specific binding to matrix proteins bound to microtiter plate surface. In the study, they also analysed the composition of protein

corona on PAA-coated UCNPs, finding that the most abundant proteins were alpha-2-HS-glycoprotein, serum albumin, and platelet factor.[185]

In a study by Nsubuga et al (2018) UCNPs were coated via the two-step ligand exchange using PEG, alendronate and o-phospho-L-tyrosine. While PEG and alendronate coated UCNPs were shown to be water soluble with no detectable protein corona in serum, some corona formation was detected on o-phospho-L-tyrosine-coated UNCPs. While the results support the usage of two-step ligand exchange, it is also shown that ligand identity does have a direct effect on non-specific binding to proteins.[7]

UCNPs may also non-specifically bind directly to solid surfaces such as polystyrene commonly used to manufacture microtitration plates, or the proteins used to coat them, and this has been shown for example by Lahtinen et al. (2018). In their study, they developed surface chemistry dependent countermeasures for the problem. As they utilized PAA-coated UCNPs, they added free PAA of smaller molecular weight to the assay buffer. Theoretically, the small PAA polymers would block the binding sites on the plate surface to prevent non-specific binding. Their results supported this hypothesis, as significant decrease in non-specific binding of reporter was observed upon addition of the free polymer. [44]

2.4.2 Microtiter plate format

Aim of utilizing upconversion in immunoassay reporters is to improve sensitivity through the high detectability, achieved by removal of autofluorescence and immense specific activity. Usability of UCNPs over other reporters in MPAs has been shown in a cavalcade of research by various groups.

Analog two-step upconversion MPAs have been of interest since their development in the 1990's. One of the earliest assays detected prostate-specific antigen on tissue sections and CD4 membrane antigen on human lymphocytes.[186] Group of Shapoval directly compared an upconversion MPA for a cardiac marker to an assay with same components but with an enzyme reporter, and reported a 12- and 2-fold improvement in sensitivity when UCNPs were used. [187] In a similar experiment, a 22-fold improvement in sensitivity by changing the reporter from an enzyme to an UCNP was reported in an assay for a honeybee disease American foulbrood.[188] A higher detection sensitivity with UCNPs compared to conventional enzyme reporters have also been reported in studies targeting carbohydrate antigen 19-9,[189] and another honeybee pathogen *Melissococcus plutonius* (400-fold improvement).[190] A publication about detection of diclofenac reached similar sensitivities with UCNPs as with a conventional ELISA, but faster due to lack of enzymatic amplification.[191] Upconversion luminescence technologies have been shown to reach similar sensitivities as commercial assays for some analytes. [44]

To better utilize the extreme detectability of UCNPs for sensitivity enhancement, digital upconversion MPAs have been researched. Cluster formation tendency of UCNPs, in case surface chemistry has not been fully optimized, can be compensated for with a digital readout system, as discussed in section 2.1.8. A 16-fold improvement in sensitivity using digital analysis compared to analog detection on upconversion immunoassays has been shown by Mickert et al. in detection of prostate-specific antigen.[147] Also for detection of SARS-Cov-2, detection of virus in lysates was improved 10-fold by changing from analog to digital readout. On the other hand, detection of wildtype N-protein was 3-fold more sensitive when changing from ELISA to upconversion-based detection, but no difference between analog and digital readout was observed.[148]

2.4.3 Lateral flow format

Upconversion luminescence LFAs (UCL-LFA) have been developed for a large number of analytes and they have shown incredible promise for both research of diseases and development of POC assays for analytes which have previously required central laboratory testing due to high sensitivity requirements.[192–194] In LFAs, effect of elimination of autofluorescence is even more pronounced than in MPAs, as the rinsing of sample matrix from the detection area may not be as efficient as the separation in MPAs. Although UCNPs require a device for readout, compromising affordability, it is compensated by the possibility to develop quantitative LFAs. Various affordable devices for POC purposes have also been described in the literature.[69,195–200] Quantitative analysis in LFAs can reduce the human error in result interpretation and enable direct archiving of results in a digital form.[201] However, it should be considered that LFAs suffer from poor reproducibility due to non-controlled environmental conditions in field use, compromising reliability of absolute quantitative results.[84] Through automated platforms, it is possible, however, to reduce sources of variation in LFAs.

A UCL-LFA for detection N-terminal fragment of B-type natriuretic peptide precursor, an acute heart failure biomarker, was shown to reach a sensitivity significantly below the clinical cut-off value, serving as evidenced for clinical usability of such an assay, and they further applied the novel technology to show age and sex dependence of the biomarker concentrations in healthy patients.[202] A 250-fold improvement for detection of *Plasmodium falciparum* malaria compared to standard tests was shown with a UCL-LFA, showing potential of revolutionizing malaria diagnostics by ability to detect asymptomatic carriers simply, affordably and on-site.[194] Improved POC detection using UCL-LFA has also been shown for hepatitis B virus surface antigen, compared to a visually read LFA.[193] A universal, smartphone-readout -based UCL-LFA platform has been developed and shown to

enable high sensitivity detection of various analytes, including small molecules, heavy metal ions, bacteria, nucleic acids and proteins.[195] A UCL-LFA has been shown to reach a similar sensitivity to a commercial assay for myoglobin.[203] In some instances, upconversion luminescence-LFAs even outperform conventional MPA-ELISAs. For example, better analytical sensitivity and accuracy was reported for an upconversion-LFA for *Schistosoma* circulating anodic antigen compared to an ELISA approach with clinical samples. [152]

To improve sensitivity of LFAs, multi-step assay formats can be used as well as pre-incubation steps of reporter with the sample before deposition onto the strip,[204] however, they are not well compatible with the POC environment. To even further improve sensitivity of POC detection besides changing into upconverting reporters, automated flow control methods have been integrated to enhance the technology without needing to add manual steps. For example, a mechanism of a standard kitchen timer was harnessed to drive different assay steps via pressing actuating balls in a timed sequence against reagent containing pouches to release their contents onto an LF-strip.[205]

2.5 Cardiac troponin I in diagnostics

2.5.1 Cardiac troponins

Cardiac troponin (cTn) complex is a component in the heart muscle is composed of three subunits I, T and C, and the function is essential in contraction of the heart.[206,207] In myocardial infarction, blood supply to the heart muscle is obstructed due to blockage of an artery. This leads to hypoxia of the muscle, initiating cell death. As the tissue suffers cellular damage, intracellular proteins are released into circulation. In the range of proteins released, cTns are ones that are entirely specific to the heart muscle. Without cardiac damage, they are present in circulation in very small quantities. Thus, the increase in cTn concentrations can be used as indication of cardiac damage. [16]

2.5.2 Clinical diagnostics

Cardiac troponin **I** (cTnI) and T (cTnT) are the current standard biochemical markers for diagnosis of cardiac injuries. Of the two, cTnI is considered more specific.[16] Proteins released into circulation after skeletal muscle injury have been shown to cross-react with cTnT assays, leading to falsely elevated results in patients when cTnT tests are used.[18,208–211] In addition, chronic kidney disease or other renal failure has been shown to be associated with increased levels of cTnT, as opposed to cTnI.[212–214] Although myocardial injury and infarction are always related to increase in cTns in circulation, electrocardiograms and patient symptoms, vital signs, history

and interviews are used to define a more specific diagnosis, including the nature of the damage and position of the possible infarction on the heart.[16] For example, highly strenuous and long-lasting athletic performance may lead to heart injury releasing intracellular components from cardiac tissue.[215]

2.5.3 Challenges in troponin testing

Although cTn-assays are routinely used in cardiac injury diagnostics, interpretation of the results is not straightforward and the numerical results vary between assays. In addition, The baseline level of cTns in healthy population varies heavily based on age and sex. [216]

The kinetics of troponin in circulation after cardiac injury is shown in Figure 7. Directly after injury, the concentration rises quickly, reaching a plateau, followed by decrease after the acute phase. Elevated troponin values usually remain detectable for days after the acute infarction. Absolute values are dependent on the assay technology and the patient, especially the age and sex, and thus the change in concentration over time (i.e. delta-value) has been studied to be a better approach in diagnostics.[217]

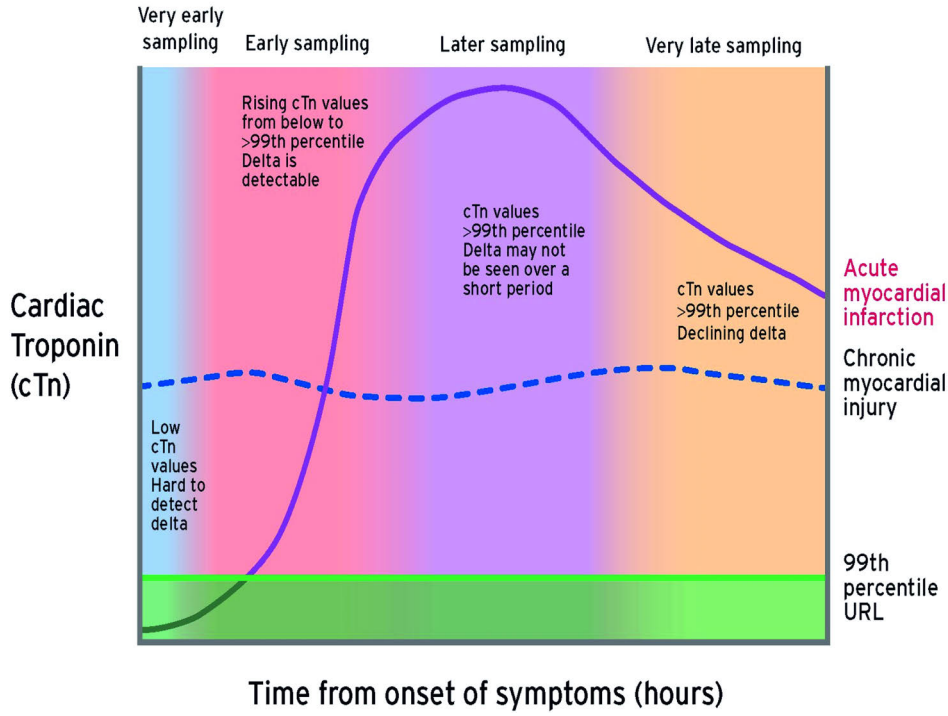

Figure 7. Troponin kinetics in cardiac injury. URL refers to upper reference limit in population. Reprinted with permission from Thygesen et al.[16]

The main reason for variance between assay technologies is lack of standardization.[16] Different assay formats give different numerical results for cTn-concentrations, because there is no standardized reference material to cTns which could be used in universal calibration of the assays. Further causes for differences between cTn assays, especially for cTnI, are caused by biochemical properties of the protein. First issue is similarity of cardiac troponin I with skeletal troponin I, as 40% of their amino acid sequence is shared.[218] Several post-translational modifications have also been found in cTnI proteins. Phosphorylation can occur by protein kinase A on either or both of two serine residues in cTnI, leading to 4 possible forms of the protein coexisting in cells, and each form has a different conformation, with all of these found among circulating cTnI.[218,219] In addition, oxidization, reduction, and digestion by proteases have been noted having occurred to TnI in circulation.[220] The mentioned modifications usually occur on the peripheral parts of the cTnI protein, leaving the central part more conserved. However, over 95% of circulating cTnI is a binary complex with troponin C, which interacts with the middle part of cTnI.[221] cTnI can also form complexes with heparin, heterophile- or anti-cTnI-autoantibodies in circulation.[66,218,219] All of these aspects and interactions lead to difficulties in specific and sensitive detection of circulating cTnI. Thus, choice of antibodies in cTnI assays needs to be done through understanding the epitope behaviour and availability on the protein, while avoiding cross-reactivity with skeletal troponin. Through assessment of hundreds of antibody combinations in cTnI assays, it has been concluded that there is no existing pair of antibodies which could detect all the forms of cTnI, and thus a combination of three or more antibodies should be utilized in cTnI assays.[222]

Thus, for all developed cTn-assays, the upper reference limit (URL) for 99th percentile, for each sex, has to be studied with the assay technology in question, and appropriate quality control materials need to be used to validate the imprecision at the URL. Reference population selection strategies have been studied to have great significance on the determined 99th percentile URL values, and also the measured sex differences.[223] Despite the difficulties, development of high sensitivity (hs)-cTn assays has been a hot topic during recent decades. hs-cTn assays are defined by two criteria: 1. Their ability to quantify cTn-values in patients at the 99th percentile cut-off value with ≤10% CV, and 2. cTn values of at least 50% of healthy population below the 99th percentile cut-off value should be quantifiable.[218,224] A third criterion has also been mentioned, specifying the LoD to be <10 ng/L. [225]

Time interval for blood sampling to calculate for the delta depends on the sensitivity of the assay used. For conventional cTn-assays, 3 h and 6 h interval can be used. However, in case of hs-cTn assays, the sampling can begin already at 1 h after onset of symptoms because delta can be calculated for smaller concentrations than with conventional assays, and the subsequent sampling interval can be reduced

to 1 or 2 hours, reducing waiting times in the emergency room and improving patient outcomes and reducing costs.[16,19,226–228]

2.5.4 Point-of-care detection of troponins

Waiting times could further be reduced by POC tests, as the turnaround time for a POC test is generally shorter than for central laboratory testing, for example simply because of lack of need for transportation of the samples. However, currently the preference is towards hs-cTn assays, and no validated POC test for cardiac injury answers to the sensitivity requirements.[229] The preference should be re-evaluated once hs-POC-cTn tests are developed, validated and brought to market.[230] Potential brought upon by development of upconverting nanomaterials in cardiac diagnostics has been recognized by pronounced cardiac experts.[231]

3 Aims of the study

The overall aim of this thesis was to study and improve the usability of UCNPs as reporters and exploit their unique properties in development of ultrasensitive immunoassays for cardiac troponin I.

The aims, differentiated by publication, are:

I To study the effect of UCNP surface chemistry, core diameter and immunoassay format using digital and analog readout modes, aiming to enhance sensitivity of cTnI detection in a microtiter plate -based assay.

II To improve the surface chemistry and further improve the assay developed in the original publication **I**. The improvements were done by minimizing the cluster formation tendency and non-specific binding of the UCNP reporter via modification of surface chemistry, and by studying the effect of all assay reagents. The final aim was to demonstrate the extreme detection sensitivity for cTnI attainable with UCNPs.

III To study the suitability of the minimally aggregating and non-specifically binding UCNP reporter in a lateral flow format, and to develop an automated ultrasensitive lateral flow assay for cTnI.

4 Materials and Methods

Key materials and methods used in the thesis research are briefly summarized in this section. For more detailed descriptions, refer to the original publications.

4.1 Synthesis of UCNPs

Upconverting nanoparticles (UCNPs; $NAYF_4$: 17% Yb, 3% Er) of approximately 25 nm and 63 nm in diameter used in original publications **I** and **II** were synthesized by high-temperature co-precipitation in organic oils under high temperature, while UCNPs of 40-80 nm in diameter were purchased from Kaivogen Oy (Turku, Finland).

4.2 Surface chemistry of UCNPs

4.2.1 PAA-coating

All UCNPs were OA capped after synthesis. They, apart from the 63 nm UCNP in original publication **I**, were rendered hydrophilic by poly(acrylic acid) (PAA) coating using two-step ligand exchange with tetrafluoroborate ligand as the intermediate. The pH when exchanging the tetrafluoroborate to PAA was adjusted to 9 using NaOH in original publication **I**, while in original publication **II**, effect of replacing NaOH with organic base 1,8-diazabicyclo(5.4.0)undec-7-ene (DBU) was studied. Use of DBU was continued in original publication **III**. The UCNPs with these surface chemistry approaches are referred to in the Results section as PAA(NaOH) and PAA(DBU) for simplicity.

4.2.2 Streptavidin-PEG-coating

In original publication **I**, the 63 nm OA-capped UCNPs were rendered hydrophilic by HCl-facilitated phase transfer from cyclohexane to water, followed by coating with self-synthesized alkyne-polyethylene glycol-nerindronate-linker (Alkyne-PEG-Ner). The Alkyne-PEG-Ner-UCNPs were further functionalized with SA using copper(I)-catalysed alkyne-azide click chemistry to yield SA-PEG-UCNPs.

4.2.3 Bioconjugation of PAA-UCNPs

In all original publications, the PAA-UCNPs were bioconjugated to anti-cTnI-antibodies (Mab 625, and in original publication **I**, also to Mab 560, both purchased from HyTest [Turku, Finland]) using standard NHS-EDC-coupling chemistry in MES-buffer of pH 6.1, to yield Mab 625-PAA-UCNPs. In original publication **I**, the concentrations of EDC and sulfo-NHS-activators were 20 and 30 mM, respectively, while in original publication **III**, the respective concentrations was 2.5 and 30 mM. In original publication **II**, the effect of EDC concentration to the monodispersity and binding efficiency was studied (see sections 4.3.2 and 4.3.4), so the used concentration was varied between 2.5-20 mM.

4.3 Characterization of UCNPs

4.3.1 Size and morphology

The synthesized OA-capped UCNPs were imaged by transmission electron microscopy (TEM-imaging) under 80 kV electron beam and 80 000 x magnification, using JEM-1400 Plus (JEOL, Massachusetts, USA). Their size was analysed from the images by an in-house program with particle recognition based on detection of different colour shades in TEM-images with manually set threshold, and desired round morphology visually confirmed from the images.

4.3.2 Monodispersity

In original publication **I**, the monodispersities of Mab-conjugated PAA-UCNPs and SA-PEG-UCNPs (sizes 40-80) in buffer were measured as their hydrodynamic diameters by dynamic light scattering (DLS) using Zetasizer Nano (Malvern, UK). In original publication **II**, monodispersity and size-distribution of aggregates in aqueous solution of PAA-coated UCNPs was evaluated via UCNP-gel electrophoresis on 0.6% agarose gel (in Tris-borate buffer pH 8.6, ran for 20 min under 150 V). The cluster formation tendency in biological fluids of Mab-conjugated PAA-UCNPs was characterized with a filtration experiment, where percentage yield of UCNPs after filtration through 0.22 and 0.1 μm pore-size filters after incubation of UCNPs in buffer or in presence of 20 % plasma.

4.3.3 Binding efficiency

In original publication **II**, binding efficiency of Mab-UCNP-reporters to the analytes bound to capture antibodies was analysed in an activity assay following the assay

protocol described in section 4.4.2, apart from using three concentrations cTnI calibrators (50; 500 and 5000 ng/L) and 10 ng/well of Mab-UCNP-reporter. The binding efficiency was calculated as concentration normalized analyte-bound fractions of the Mab-UCNPs added in the well.

4.4 Microtiter plate assays for cTnI detection

4.4.1 SA-PEG-UCNPs in digital microplate assays

In original publication **I**, transparent bottom 96-well microtiter plates (µClear, Greiner Bio-One, Kremsmünster, Austria) were coated with anti-cTnI Mabs 19C7cc and MF4cc (HyTest Oy). The assay was conducted by first washing and blocking the plate by incubation with SuperBlock (ThermoScientific, Waltham, MA, USA) in TBS buffer (supplemented with 1 mM KF, 0.05% Tween-20, 0.05% PEG and 0.05% NaN_3, pH 7.5) for 1 h, followed by washing and addition of troponin I-T-C standard (HyTest Oy) calibrators or plasma samples (20 % of I-T-C-spiked plasma) in 60 µl of BSA-Bovine gamma globulin buffer (BSA-BGG; 37.5 mM Tris, 513 mM NaCl, 5% D-trehalose, 2.5% BSA, 0.06% BGG). After 1 h incubation time and washing, the captured analytes were detected by incubation for 1 h of Mabs 560cc and 625cc (in ratio 1:1, 1 µg/ml in total) in 60 µl of SuperBlock in TBS with 5 mM CaCl2 and washing. Labeling was done subsequently by addition of SA-PEG-UCNPs (6.5 µg/ml in 60 µl SuperBlock in TBS with 5 mM $CaCl_2$) and incubating for 1 h, followed by washing. Before measurement, the plates were airdried. Assay format is illustrated in Figure 8a.

4.4.2 PAA-UCNPs in digital and analog microplate assays

In original publication **I**, transparent bottom microtiter plates, and in **II**, white microtiter plates were coated with 1 µg SA/well and blocked with BSA. Half-an-hour before start of assay, Mab 625-PAA-UCNPs were diluted to modified assay buffer (Kaivogen assay buffer [Kaivogen Oy, Turku, Finland] supplemented with 1 mM KF, 0.05% PAA [Mw 1200], 0.2% fat-free milk powder, 0.08% native mouse IgG and 0.005% denatured mouse IgG) to correspond 200 ng/50 µl.

Assay started by prewashing the plate and incubating 200 ng/well biotinylated capture in commercial assay buffer in rotation, room temperature, 900 rpm. The capture antibodies were a combination of 75% Mab 19C7 and 25% Fab 9707 site-specifically biotinylated while expressed hybridoma cells (in original publication **I**), or 50% Mab 19C7 (HyTest Oy) and 50% Mab 9707 (Medix Biochemica, Espoo, Finland) (in original publication **II**).

Calibrators (cTnI diluted to 7.5% BSA-TSA buffer pH 7.5) and I-T-C-spiked plasma samples were diluted ¼ in BSA-BGG buffer (in original publication **I**) or ¾ in BSA-BGG buffer (in original publication **II**). They were added to plate in total volume of 50 µl/well and incubated in a similar manner as capture antibodies.

Labelling was done after washing the plate by addition of 200 ng of UCNP-reporters in 50 µl/well and incubated for 15 minutes in room temperature at 900 rpm shaking. Unbound reporter was washed with Kaivogen wash buffer in original publication **I** and Kaivogen wash buffer with pH adjusted to 10.25 in original publication **II**, and plate was allowed to airdry before measurement. Assay format is illustrated in Figure 8b.

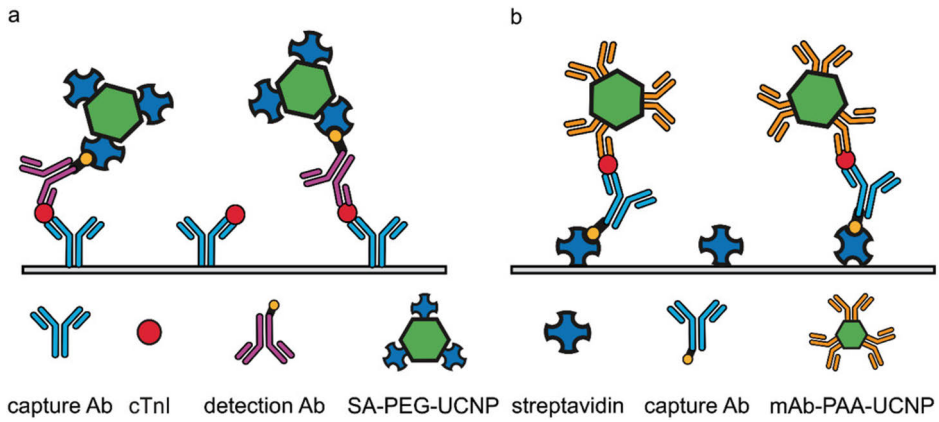

Figure 8. Illustration of assay format where **a)** SA-PEG-coated UCNPs were used to label a detection antibody bound to cTnI, immobilized via capture antibodies passively adsorbed to plate surface (used in original publication **I**), or **b)** Mab-PAA-UCNPs were used to detect cTnI bound to a biotinylated capture antibody immobilized on plate surface via passively adsorbed streptavidin (used in original publications **I** and **II**). Figure reproduced with permission from original publication **I**.

4.5 Lateral flow assays for cTnI detection

4.5.1 Preparation of lateral flow strips

Test lines (1000 ng/cm of Mab-19C7, Mab-916 and Mab-9707 in ratio 1:1:0.5) and control lines (600 or 1000 ng/cm rabbit-anti-mouse) in printing buffer (10 mM Tris pH 8, 5% EtOH, 1% Sucrose, 40 µg/ml cherry red) were printed on 25 mm wide nitrocellulose (LFNC-C-BS023-70, Nupore Filtration Systems Pvt. Ltd., Ghaziabad, India) with Linomat 5 printer (Camag, Muttenz, Switzerland). Lines were printed 5 mm apart and the test line was 10 mm from the front end of the nitrocellulose, followed by overnight drying in 35 °C. The nitrocellulose with printed lines, a glass fibre sample pad (16 mm wide, saturated with 10 mM borate buffer pH 7.5, 0.1%

Tween-20, 0.5% BSA, 50 mM EDTA and dried), and 34 mm wide cellulose absorbent pad were attached on backing cards with approximately 1 mm overlap, and 4.8 mm wide LF-strips were cut.

4.5.2 Reference assay

Reference assay followed a dipstick format published previously. [204] In short, plasma (pooled human plasma collected from volunteers in following the Declaration of Helsinki[232]) was thawed, purified from agglutinated proteins by centrifuging 3000 rpm for 10 min, and spiked with recombinant troponin ITC complex (HyTest) to concentrations of 0.5-500 ng/L cTnI. Samples (25 µl) were pre-incubated with 100 ng Mab625-PAA-UCNP reporters (in 25 µl of assay buffer [0.05 M Tris pH 7.5, 0.5 M NaCl, 0.04% NaN3, 2 mM KF, 1.5% BSA, 0.06 % bovine gamma-globulin, 0.2 mg/ml mouse IgG, 0.05 mg/ml denatured mouse IgG, 0.05% PAA Mw 1200]) in 900 rpm shaking, 35 °C for 15 minutes before application on strips. After 9 minutes, 50 µl of assay buffer was added to conduct a wash step. UCL signal was scanned 40 min since application of sample.

4.5.3 Fabrication of actuation device

The device is depicted in Figure 9. Computer Assisted Designing software Autodesk Inventor Professional 2021 (Autodesk Inc. Mill Valley, California, USA) was used to design the 3D-printed parts and convert them to .stl-files. For slicing, Prusa Slic3r Version 2.3.3.+win64 (Prusa Research by Josef Prusa) was used. Parts were printed using polylactic acid filament on Original Prusa i3 MK3S 3D-printer. All other parts but a standard mechanical kitchen timer mechanism and three metal screws, along with 200 µl PCR-tubes, were 3D-printed. For details of assembly, see original publication **III**. Holes were punched at the bottom of PCR-tubes using a 3D-printed tool to control the puncture position, equipped with a 0.9 mm needle.

4.5.4 Actuator mediated assay

An LF-strip was placed in the actuator device. Plasma samples and wash buffer were as described in section 4.5.2, but assay buffer for Mab625-PAA-UCNPs reporter dilution was optimized for the actuator assay (0.15 M Tris pH 7.5, 1.5 M NaCl, 0.04% NaN_3, 2 mM KF, 4.5% BSA, 0.18% bovine gamma-globulin, 0.6 mg/ml mouse IgG, 0.15 mg/ml denatured mouse IgG, 0.3 % PAA Mw 1200). Deposition tubes were placed in tube holders and 25 µl of plasma sample was pipetted with 100 ng of reporter in 5 µl of optimized buffer were pipetted to sample tube, and 50 µl of assay buffer was pipetted to wash buffer tube. Actuator was rotated to position of 50

minutes on the timer scale. The reporter and sample were deposited by the actuator after 15-minute incubation in the tube, followed by deposition of wash buffer 5 minutes later. When the bell rang, the strip was measured.

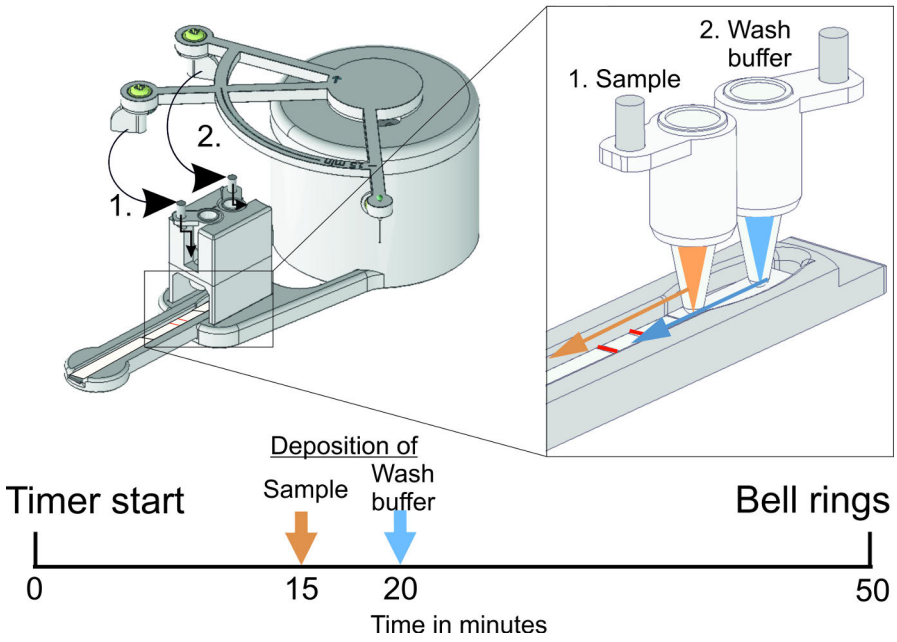

Figure 9. Actuator method of function. Sample and reporter are incubated together for 15 minutes in the first tube, after which the first paw of the actuator knocks down the tube to establish contact with the hole at the bottom of the tube and the sample pad, starting the flow. Five minutes later, wash buffer is deposited by second paw of the device in the same manner.

4.6 Assay readouts

The digital readout in original publication **I** was conducted in University of Regensburg (Germany) using an inverted wide-field epifluorescence microscope, connected to a continuous-wave 980 nm laser diode (4 W) via a multimode optical fibre (105 µm fibre core, 0.22 NA) and a motorized TIRF/Epifluorescence illuminator unit. Nine wide-field images per well were captured, 166 × 144 µm2 each, from all the wells and the number of UCNPs/well was analysed using a four-parameter logistic function.

In original publications **I** and **II**, a modified upconversion microtiter plate reader[119] equipped with a 980-nm laser excitation source was used for measuring the UCL. For SA-PEG-UCNP-reporters, 8 x 8 raster with points at 100 µm distance using 1 s integration time was measured, followed by calculation of truncated average intensity (16 highest and lowest values discarded) for each well. In case of

Mab 625-PAA-UCNPs, the average signal of each well was calculated based on 3 x 3 raster scan with 1.5 mm step size and 2 s integration time.

UCL signal from the lateral flow strips in original publication **III** was measured with UPCON-reader (Labrox, Turku, Finland) using 976 nm excitation and 540 nm emission wavelengths, scanning 125 points over 25 mm range along the middle of the strip (spanning test and control lines) with 1 mm emission spot size measuring 100 ms/spot.

4.7 Assay performance analysis

In all original publications, average signals and standard deviations of three replicates at minimum were calculated and used to plot analyte specific signals. Data was fitted by a four-parameter logistic function. LoDs were calculated according to the IUPAC-definition as three times the standard deviation of the non-spiked sample in original publications **I** and **III**, while in **II** the LoD was calculated based on the CLSI guideline EP17-A2, comprising of four low cTnI-level plasma samples assayed in four replicates over four days, leading to parametric analysis of 64 replicates. The limit of blank was determined using non-parametric analysis of 60 replicates of non-spiked plasma samples. Within-and between-run precisions were calculated based on five assay repeats comprising of four replicates of each concentration. Recovery percentages were calculated by quantifying four replicates of spiked pooled plasma for the dynamic range concentrations. Calculated concentration of non-spiked plasma was reduced from the spiked plasma concentrations. Assay performed in original publication **II** was also validated via reference assay by quantifying the cTnI-concentrations of identical aliquots of I-T-C-spiked plasma in the range of 0-250 ng/L with both assays.

5 Results and discussion

5.1 Characterization of UCNPs

5.1.1 TEM-imaging

In all original publications, the non-functionalized UCNPs were mostly spherical in morphology with narrow size distributions (Figure 10). The commercial UCNP cores used in original publication **I** (9.b-f) exhibited more angled or cubic shapes with increasing core size.

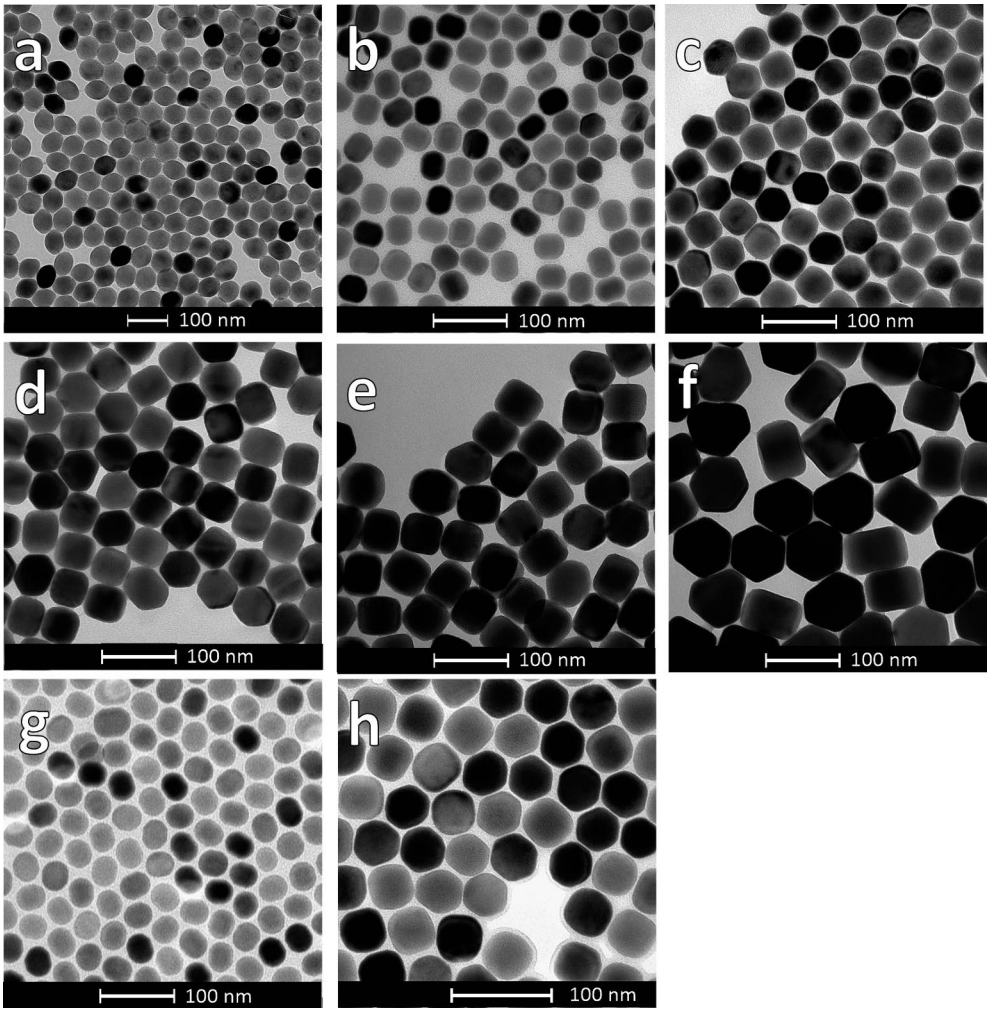

Figure 10. Transmission electron microscopy images of non-functionalized **a)** 64 nm UCNP-cores synthesized by co-precipitation in organic oils (original publication **I**) **b-f)** commercial UCNP-cores of sizes 40; 48; 56; 64 and 80 nm (original publication **I**), **g)** 25 nm UCNP-cores synthesized by co-precipitation in organic oils (original publication **II**), and **h)** 56 nm commercial UCNP-core (original publication **III**).

5.1.2 Effect of PAA-coating conditions

In original publication **I**, the monodispersity of bioconjugated UCNPs was characterized via DLS. The results showed narrow size distribution for all UCNPs despite size of core or surface chemistry approach. [233]

In original publication **II,** the effect of base used in pH-adjustment of PAA-coating reaction to the monodispersity of PAA-coated UCNPs was studied via UCNP-gel electrophoresis. PAA-coated UCNPs have a net negative surface charge

and thus they migrate in agarose gels in response to an electric field, and the distance travelled inside the gel is inversely correlated with the size of particle clusters. A proportionally larger number of PAA(DBU)-UCNPs travelled the maximum distance on the gel compared to PAA(NaOH)-UCNPs (Figure 11a). This indicates that using DBU instead of NaOH yields more monodisperse UCNPs.

This finding is also supported when the UCNPs were bioconjugated to antibodies and compared in a MPA for cTnI, as the UCNPs coated in presence of DBU yielded higher signals compared to using NaOH (Figure 11b). Higher signal level can be due to higher molar concentration of UCNPs (higher number of separate reporters in the same mass of UCNPs) partaking in the detection, as well as reduced steric hindrance when a reporter unit does not contain that many UCNPs aggregated together. [234] Usability of the developed PAA(DBU)-UCNPs after bioconjugation was demonstrated also in a dipstick-LFA for cTnI where they were compared to UCNPs with the same core but with a commercial carboxyl surface (Figure 11.c-d). The flow properties of PAA(DBU)-UCNPs were excellent with very low level of UCL background fluctuation and negligible amount of non-specific binding without compromising the signal response, compared to the commercial carboxylated UCNPs with the same core.

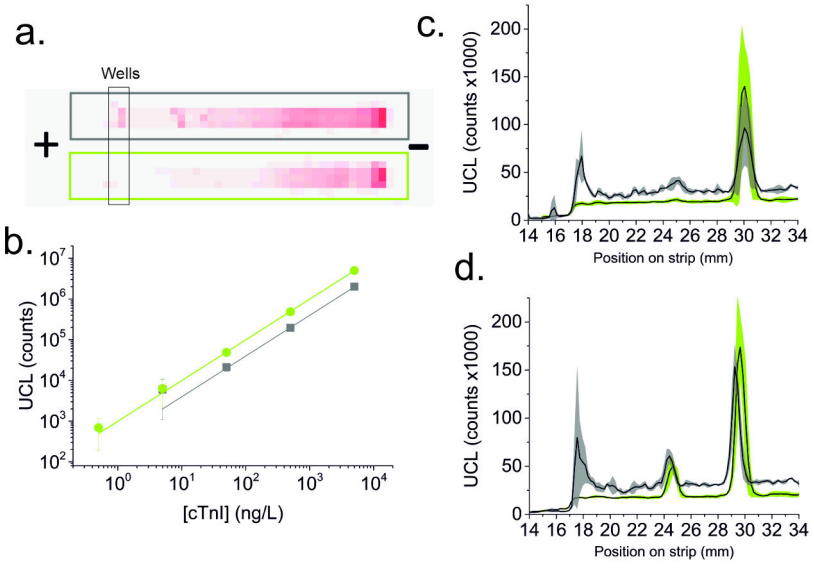

Figure 11. The effect of PAA-surface on the monodispersity and usability of UCNPs in assays. **a)** UCL intensity graph of an electrophoresis gel with PAA(NaOH)-UCNPs (grey rectangle) and PAA(DBU) UCNPs (green rectangle). **b)** Calibration curve of an MPA with either Mab 625-PAA(NaOH)-UCNPs (grey) or Mab 625-PAA(DBU)-UCNPs (green). Datapoint for 0.5 ng/L cTnI calibrator of NaOH-curve is hidden by the corresponding datapoint of DBU-curve. **c)** LFA strip UCL scanning profiles of three replicate strips with 0 ng/L cTnI. Dark line represents the average signal and the shadow the standard deviations of the replicates, assayed with Mab 625-PAA(DBU)-UCNPs (green) or Mab625-commercial-COOH-UCNPs (grey). **d)** same as **c.** but with 500 ng/L cTnI sample.

5.1.3 Effect of bioconjugation conditions

The effect of EDC-concentration used in bioconjugation to monodispersity of anti-cTnI Mab 625 bioconjugated UCNPs was studied by filtration experiments, between 2.5-20 mM EDC used in the conjugation reaction. Yield of UCNPs after filtration with 0.22 µm and 0.1 µm pore size syringe filters after incubation of UCNPs in either buffer or plasma was measured. Results showed that the filtration yield of bioconjugated UCNPs increased significantly with decreasing EDC-concentration in the conjugation reaction, and the effect was noticeable after filtration with 0.1 µm pore size filter after incubation both in buffer and in presence of plasma, throughout the range of used EDC-concentrations (Figure 12).

Binding efficiency of UCNPs to cTnI in an MPA was determined for UCNPs conjugated with 2.5-30 mM EDC concentrations in the reaction. A clear, almost linear inverse proportionality was observed between binding efficiency and EDC-concentration (Figure 12).

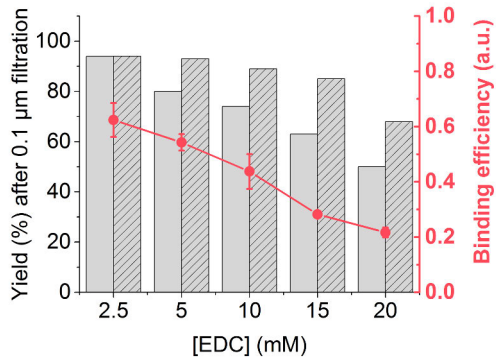

Figure 12. Effect of EDC-concentration used in bioconjugation reaction on monodispersity of Mab 625-PAA(DBU)-UCNPs, evaluated by calculating the percentage yield after filtration with 0.1 µm filter, after incubation in either buffer (grey bars) or buffer with 20% plasma (striped bars). Binding efficiency of the conjugates is shown as a red line, with error bars corresponding to standard deviations of three replicates.

5.2 Evaluation of upconversion luminescence assays for detection of cTnI

A summary of LoDs achieved with different UCNPs on different assay technologies and antibody combinations in buffer or in plasma is presented in Table 1.

Table 1. Summary of achieved sensitivities.

Publication	UCNP synthesis	UCNP ⌀ (nm)	Surface chemistry	Assay technology	Antibody combination (detection/capture)	Lod in buffer (ng/l)	LoD in plasma (ng/l)	LoD determination
UNPUBLISHED	In-house	25	PAA (NaOH)	MPA analog	625 / 19C7 + Fab 9707	2.2	0.56	IUPAC
I	In-house	63	SA-PEG	MPA analog[1]	560 / 19C7 + MF4	41	30	IUPAC
I	Purchased	48	PAA (NaOH)	MPA analog[1]	625 / 19C7 + Fab 9707	3.8	8.6	IUPAC
I	Purchased	56	PAA (NaOH)	MPA analog[1]	625 / 19C7 + Fab 9707	8.3	11.8	IUPAC
I	Purchased	64	PAA (NaOH)	MPA analog[1]	625 / 19C7 + Fab 9707	13.3	57.2	IUPAC
I	Purchased	80	PAA (NaOH)	MPA analog[1]	625 / 19C7 + Fab 9707	2.9	44.9	IUPAC
I	In-house	63	SA-PEG	MPA digital	560 / 19C7 + MF4	19	31	IUPAC
I	Purchased	48	PAA (NaOH)	MPA digital	625 / 19C7 + Fab 9707	3.3	9.8	IUPAC
I	Purchased	56	PAA (NaOH)	MPA digital	625 / 19C7 + Fab 9707	7.0	65.2	IUPAC
I	Purchased	64	PAA (NaOH)	MPA digital	625 / 19C7 + Fab 9707	17.4	17.2	IUPAC
I	Purchased	80	PAA (NaOH)	MPA digital	625 / 19C7 + Fab 9707	4.7	160	IUPAC
II	In-house	25	PAA (NaOH)	MPA analog	625 / 19C7 + 9707	2.7	-	IUPAC
II	In-house	25	PAA (DBU)	MPA analog	625 / 19C7 + 9707	12	-	IUPAC
II	In-house	25	PAA (DBU)	MPA analog	625 / 19C7 + 9707	-	0.06 / 0.13	IUPAC[2] / CLSI EP17-A2
UNPUBLISHED	Purchased	56	PAA (NaOH)	Dipstick LFA	625 / 916 + 19C7 + 9707	-	19.1	IUPAC
UNPUBLISHED	Purchased	80	PAA (NaOH)	Dipstick LFA	625 / 916 + 19C7 + 9707	-	18.1	IUPAC
UNPUBLISHED	Purchased	78	Commercial COOH	Dipstick LFA	625 / 916 + 19C7 + 9707	-	19.5	IUPAC
UNPUBLISHED	In-house	25	PAA (DBU)	Dipstick LFA	625 / 916 + 19C7 + 9707	-	140.5	IUPAC
III	Purchased	45	PAA (DBU)	Dipstick LFA	625 / 916 + 19C7 + 9707	-	7.6	IUPAC[3]
III	Purchased	45	PAA (DBU)	Automated LFA	625 / 916 + 19C7 + 9707	-	1.5	IUPAC[3]

[1]Clear plates. IUPAC LoD[235] is determined with 6 replicates of blank for MPAs and 9 for LFAs, apart from [2]with 60 and [3]with 12. Antibodies used are Mab unless otherwise specified.

5.2.1 UCNP size and analog and digital detection

The method where in house synthesized 63 nm SA-PEG-coated UCNPs were used, generally resulted in poorer sensitivity in both buffer and plasma, as well as in digital and analog detection, than with UCNPs of similar size in the sandwich format using PAA-Mab-coated UCNPs. This result implies that the assay format with streptavidin immobilized capture on the bottom of the well, as opposed to streptavidin conjugated UCNPs, results in higher sensitivity in UCL-based cTnI detection. This can partly be attributed to 10-fold difference in non-specific binding observed in digital measurements (original publication **I**). The surface chemistry or the assay format, or both, seem to have a more significant effect on the sensitivity of the assay than the readout mode. With the size series of PAA-Mab-coated UCNPs, the readout mode no clear effect on the sensitivity either. Although reduction of non-specific binding generally improves sensitivity, in digital detection, the less counts (n) to measure, the higher the mathematical Poisson noise ($\sqrt{n}/n$), which is a determining factor in uncertainty of digital assays.

Imaging based digital detection requires extreme detectability, which in theory, is provided by UCNPs of sufficient size. For 25 nm and 40 nm UCNPs, digital detection was not possible due to too low luminescence intensity. However, with larger size, the surface area for non-specific interactions between the particle and the solid surface increases as well, leading to increased non-specific binding. The increase in background signal with increasing UCNP size was recorded in the assays (original publication **I**). Digital detection has been shown to improve sensitivity with UCNP MPAs in previous research, but the effect has been discussed most notable with highly aggregated UCNPs.[147] It is possible that the UCNPs applied in this research were monodisperse enough to function adequately in analog detection, so the digital detection did not bring significant improvement over the analog. In fact, when the 25 nm in-house prepared UCNP, with similar surface chemistry, antibodies and assay setup as the size series, is assayed on white microtiter plates, the sensitivity surpasses all those with analog or digital detection on transparent-bottom plates. This attributes the sensitivity improvement more towards the ability to gather as much of the luminescence to the detector as possible, rather than individual observation of the particles, in addition to using a UCNP with smallest diameter, i.e. smallest surface area for non-specific binding.

5.2.2 Surface chemistry and sensitivity

The PAA-Mab-surface and the corresponding assay format, which enabled the best sensitivity in original publication **I**, were utilized in further research. The surface chemistry approach was improved by changing the pH adjusting agent in the PAA-coating reaction from NaOH to DBU, yielding more monodisperse UCNPs (original

publication **II**). Combining NaOH with sodium acrylate is a common method of synthesizing super absorbent polymers through polymerization. Polymerization of PAA during the reaction in presence of NaOH is supported by visible sticky pellet formation, which can lead to poor coverage of the UCNPs when PAA is removed from the solution, or even aggregation through polymerization of PAA-molecules on UCNP surface. Changing the pH adjusting agent in UCNP coating lead to over 4-fold improvement in sensitivity when the UCNPs were applied in a microplate immunoassay for cTnI. This may be attributed to improved monodispersity in two ways. First, as the UCNPs are dispensed in the assay based on mass, there is a smaller number (smaller molar amount) of reactive reporters participating in detection, if the UCNP stock is heavily clustered. Secondly, large clusters have a large surface area, and thus a larger probability to non-specifically bind to surfaces. As the improvement was noted in analog detection, a large non-specifically bound aggregate may significantly affect background signal, undermining sensitivity. Relationship between monodispersity and reactivity of the reporter was further supported in optimization of EDC-concentration in bioconjugation, as the decrease in cluster formation tendency lead to increase in binding efficiency (section 5.1.3 Effect of bioconjugation conditions).

In addition to reporter properties, the assay was improved. Various different brands of streptavidin were studied, and surprisingly large differences in non-specific binding of UCNPs was measured depending on the brand. The optimal ratio of capture antibodies was studied and the antibody binding fragment of 9707 was changed to the full antibody type of the same binder. In addition, the improved surface chemistry and increasing wash buffer pH up to 10.25 in the last washing step lead to decrease of non-specific binding in assays using plasma, enabling the increase of spiked plasma sample volume from 20% to 80% in relation to assay buffer, further improving sensitivity of detection.

Different sized UCNPs with different surface chemistries were also studied in an LFA. The 25 nm UCNP with PAA(DBU)-Mab-surface, which showed best performance in MPAs, showed poorest performance in LFA with LoD of 140 ng/L, compared to 56-80 nm UCNPs with either PAA(NaOH)-surface or a commercial carboxyl surface, all of which performed almost similarly to each other with LoDs of around 20 ng/L. The poorest sensitivity of the 25 nm UCNP is attributed to the dimness, as the luminescence levels in the assays were 10-fold weaker than with commercial core UCNPs. However, the scanned UCL profile of the strips showed exceptionally minimal background luminescence fluctuations, which implied excellent suitability of the surface chemistry on the 25 nm UCNP (PAA[DBU]) compared to the PAA(NaOH) and the commercial carboxyl surface. The LoD achieved when commercial bright 45 nm UCNP core was coated using the

PAA(DBU) approach was 10-fold better compared to any other combination of core and surface chemistry.

Currently the best commercial hs-cTnI assay systems on the market have sensitivities in the range of 1-10 ng/L in plasma.[236] Utilizing the PAA(DBU) surface chemistry approach on UCNPs, sensitivities of same or even smaller range of cTnI in plasma can easily be detected with conventional microtiter plate or even lateral flow assay setups.

5.2.3 Automation of lateral flow

High sensitivity UCL-LFA for cTnI detection was developed in previous research.[204] However, the excellent sensitivity required incorporation of a 15 minute pre-incubation step in heating, as well as a manual washing step to reduce UCL noise in the strip scanning profiles. First improvement to the previous approach was introduction of the improved UCNP surface chemistry, which allowed for reduction of the background UCL noise. Secondly, an automated device motorized by a kitchen timer (Figure 9) was developed to automate the process. Through automation, sample deposition position was fixed to minimize contamination of wash buffer with UCNPs on the sample pad. Combining the motorized device with the improved surface chemistry allowed high sensitivity detection of cTnI on LF platform with amount of manual labour corresponding to a standard LFA. Although the total time in the assay exceeds 20-30 minutes, usually considered appropriate for an LFAs, the automation system minimizes the hands-on time and simplifies the manual labor to the level of a standard one-step LFA.

6 Conclusions

UCNPs have increasingly attracted attention as assay reporters in the past couple of decades due to their excellent detectability arising from the possibility to spectrally eliminate autofluorescence in luminescence measurements. Thus, they have the potential to enable ultrasensitive immunoassays. Their widespread use has been hindered, however, by their tendency to non-specifically bind to solid supports and to each other, forming nanoparticle clusters. In immunoassays, these features lead to variation in results, undermining the theoretically extreme sensitivity of detection. In lateral flow formats, flow of different sized aggregates on the nitrocellulose membrane also leads to background luminescence fluctuations, leading to small analyte concentrations being more difficult to distinguish.

In this thesis research, aggregation and non-specific binding of UCNPs was successfully reduced by altering the surface chemistry, and combining the results with meticulous studying of all assay components possibly leading to non-specific interactions.

High sensitivity detection of cTnI has been a topic of interest in diagnostic research, as in diagnostics of myocardial infarction, the more sensitive the assay the faster the condition can be tested, improving prognosis of the rapidly progressing life-threatening state. In this research the usability of UCNPs in extremely sensitive detection of cTnI was demonstrated in both microtiter plate and lateral flow -based assays. Through UCNPs, unprecedented sensitivity in cTnI detection could be possible in rapid and simple assay setups, easily transferrable to central laboratories, or even in POC applications.

The main conclusions based on the original publications are:

I: In this research, it was shown that with monodisperse enough UCNPs and low enough non-specific binding, digital readout poses no direct improvement in limits of detection. Also, valuable information regarding the effect of biochemical format of cTnI assays and UCNP surface chemistry, as well as UCNP size, to the assay sensitivity was obtained in the research.

II: UCNPs were shown to enable a microplate immunoassay for cTnI detection of unprecedented sensitivity, after successfully minimizing UCNP aggregation and non-specific binding through surface chemistry optimization and research of all assay components. Limit of detection (0.13 ng/L) surpassed most of the commercial cTnI platforms on the current market, while reaching a level unprecedented in standard analog MPAs. The publication also highlights the significance of studying the effect of even the manufacturer of the most generic assay components, such as SA, to reach extreme sensitivities.

III: PAA (DBU) surface chemistry approach developed in original publication **II** was shown to be highly compatible with LF-applications in addition to microtiter plate format. Using the monodisperse UCNPs with minimized non-specific binding, an automated UCL-LFA was developed for ultrasensitive detection of cTnI, with no more manual steps as a standard optically read LF-test. The 3D-printed automation system combined with the UCNP-conjugates yielded an LoD of 1.5 ng/L, corresponding to a 5-fold improvement in sensitivity compared to the manual dipstick method.

Development of a surface chemistry protocol reproducibly yielding monodisperse UCNP-conjugates with minimized non-specific binding advances their use as immunoassay reporters. This was shown in three different immunoassay technologies in detection of cTnI. This thesis research yielded extremely valuable novel information regarding use of UCNPs as immunoassay reporters. Unlike often discussed, switching from analog to digital readout does not always bring about improvements in assay sensitivity, but size, brightness and surface chemistry of UCNP reporters were shown to have greater effect. In fact, when using UCNPs exhibiting low enough non-specific binding, the decreased number of events in blank wells results into Poisson noise becoming the sensitivity-limiting factor. This being established, an analog assay following a standard two-step sandwich assay workflow was developed to be combined with the novel UCNP-conjugates. The revolutionary aspect was that the extreme sensitivity was achieved in a standard microtiter plate format, because such an assay can be upscaled and converted to standard diagnostic laboratory use with relative ease, compared to the niche digital assay technologies previously reaching similar sensitivities for cTnI.

Lastly, the need for high-sensitivity POC assays has been established in review articles discussing the future cardiac diagnostics.[229,231,237,238] As the improved UCNP-conjugates were concluded to exhibit excellent flow properties on nitrocellulose, a 3D-printed actuation system was devised to automate the laborious multi-step cTnI LFA. The developed technology fulfils many of the ASSURED criteria; affordability, sensitivity, specificity and user-friendliness.[239–241]

Deliverability could be enhanced by product development as the proof-of-concept has been established here.

As the POC compatible UCL-LFA system reached a limit of detection corresponding to those of current commercial cTnI platforms used in central laboratories, the research brings POC-cTnI-assays a step closer to reality.

Acknowledgements

This research was conducted at the Biotechnology unit of the Department of Life Sciences in University of Turku during 2020-2023. I gratefully acknowledge the funding from Doctoral Programme in Technology (DPT), as well as Business Finland for funding a great portion of the research projects this research has taken place in.

I wish to thank professors the Biotechology unit, Professor Tero Soukka, Professor Urpo Lamminmäki and Associate Professor Saara Wittfooth for granting me the opportunity to work and research at this unit, and their daily endeavor to improve the department.

I would like to express my gratitute especially to my Principal supervisor, Professor Tero Soukka. He has believed in my potential since the day he hired me into his project when I was a Master's student at the unit. Since then, he has always had the time to answer my questions, handed me unique opportunities, and enabled my growth and constant improvement.

My other supervisors, PhD Teppo Salminen, PhD Iida Martiskainen, and PhD Satu Lahtinen, have truly earned my deepest gratitude for the work they've done to advance my studies and research. Their expertise and encouragement have not only been a key factor in my advancement to this point on my career, but also helped to develop my professional self-esteem and belief that I am capable, and up for this challenge.

I would also like to thank the members of my advisory committee, PhD Henna Päkkilä and PhD Terhi Riuttamäki, for their professional insight. I am also thankful for the enlightening and useful comments of the esteemed pre-examiners of my thesis, PhD, Docent Harri Siitari and Professor Laura Anfossi.

My deepest gratitude goes to the co-authors of my original publications: Julian Brandmeier, Associate professor Zdeněk Farka, PhD Riikka Peltomaa, PhD Matthias Mickert, PhD Antonín Hlaváček, Professor Petr Skládal, Associate Professor Hans-Heiner Gorris, Annika Lyytikäinen, Miikka Ekman, Aleksi Nokelainen, Oskari Nääjärvi, Sonja Koskela, PhD Iida Martiskainen, PhD Teppo Salminen, and Professor Tero Soukka. Science is a shared effort, and without all of your contribution, I would not be writing this dissertation. I would especially like to

acknowledge the contribution of Miikka Ekman in the everyday labwork. His skill to seek and combine knowledge, and always find the key details to pay attention to, have been an indispensable resource. In addition, I would like to acknowledge the substantial contribution of Saara Kuusinen. She has been there for me every day in the office and the lab, as well as our awesome work-, education- and leisure-related trips abroad. She has readily helped me with problems no matter the topic, whether it be scientific, IT-, or University bureaucracy-related, while becoming a dear friend to me in the process.

I also want to thank all my other colleagues at the Biotechnology unit, who I've had the privilege to share the lab and lunch room with. All of you have contributed to making the department feel like another home. My special thanks goes to PhD Tuomas Huovinen, whose belief in me many years ago was the spark that lead to the academic path I am on now. I would also like to thank Teija Luotohaara, Jari Vehmas and his predecessor Jani Koskinen, and Marianna Boundouvis and her predecessor Paula Holmberg, for always being up to date with their duties and keeping everything running smoothly at the lab and the unit.

Even while being surrounded by the best group of colleagues I could hope for, I could not have reached this milestone without my dear friends Julia and Kristina. No matter the problem, following Julia's advice has always led me the right way, and Kristina's positivity and energy has never failed to inspire me. Both of you have believed in me and supported me, while making sure I remember to forget about work every now and then. I would also like to acknowledge the importance of my two beloved cats, who also seem to know what is good for me, better than myself.

Lastly, I want to thank my Mom for always accepting me and giving her full support and encouragement to pursue my dreams, and my brother, who I can count on to always be on my side.

Turku, August 2023

Kirsti Raiko

List of References

1. "Principles of Competitive and Immunometric Assays (Including ELISA)", In *The Immunoassay Handbook - 4th Edition*, 4th Edn., Elsevier, 29–59 (2013).
2. Auzel. F., Upconversion and Anti-Stokes Processes with f and d Ions in Solids, *Chem. Rev.*, **104**, 139–174 (2004).
3. Haase. M. and Schäfer. H., Upconverting Nanoparticles, *Angew. Chem. Int. Ed.*, **50**, 5808–5829 (2011).
4. Hemmilä. I., Dakubu. S., Mukkala. V. M., Siitari. H., and Lövgren. T., Europium as a label in time-resolved immunofluorometric assays, *Anal. Biochem.*, **137**, 335–343 (1984).
5. Siitari. H., Hemmilä. I., Soini. E., Lövgren. T., and Koistinen. V., Detection of hepatitis B surface antigen using time-resolved fluoroimmunoassay, *Nature*, **301**, 258–260 (1983).
6. Farka. Z., Juřík. T., Kovář. D., Trnková. L., and Skládal. P., Nanoparticle-Based Immunochemical Biosensors and Assays: Recent Advances and Challenges, *Chem. Rev.*, **117**, 9973–10042 (2017).
7. Nsubuga. A., Sgarzi. M., Zarschler. K., Kubeil. M., Hübner. R., Steudtner. R., Graham. B., Joshi. T., and Stephan. H., Facile preparation of multifunctionalisable "stealth" upconverting nanoparticles for biomedical applications, *Dalton Trans.*, **47**, 8595–8604 (2018).
8. Lahtinen. S., Krause. S., Arppe. R., Soukka. T., and Vosch. T., Upconversion Cross-Correlation Spectroscopy of a Sandwich Immunoassay, *Chem. – Eur. J.*, **24**, 9229–9233 (2018).
9. Muhr. V., Wilhelm. S., Hirsch. T., and Wolfbeis. O. S., Upconversion Nanoparticles: From Hydrophobic to Hydrophilic Surfaces, *Acc. Chem. Res.*, **47**, 3481–3493 (2014).
10. Sedlmeier. A. and H. Gorris. H., Surface modification and characterization of photon-upconverting nanoparticles for bioanalytical applications, *Chem. Soc. Rev.*, **44**, 1526–1560 (2015).
11. Peltomaa. R., Benito-Peña. E., H. Gorris. H., and C. Moreno-Bondi. M., Biosensing based on upconversion nanoparticles for food quality and safety applications, *Analyst*, **146**, 13–32 (2021).
12. Gorris. H. H. and Resch-Genger. U., Perspectives and challenges of photon-upconversion nanoparticles - Part II: bioanalytical applications, *Anal. Bioanal. Chem.*, **409**, 5875–5890 (2017).
13. Mendez-Gonzalez. D., Lopez-Cabarcos. E., Rubio-Retama. J., and Laurenti. M., Sensors and bioassays powered by upconverting materials, *Adv. Colloid Interface Sci.*, **249**, 66–87 (2017).
14. Selva Sharma. A., Marimuthu. M., Varghese. A. W., Wu. J., Xu. J., Xiaofeng. L., Devaraj. S., Lan. Y., Li. H., and Chen. Q., A review of biomolecules conjugated lanthanide up-conversion nanoparticles-based fluorescence probes in food safety and quality monitoring applications, *Crit. Rev. Food Sci. Nutr.*, **0**, 1–31 (2023).

15. Kang. D., Jeon. E., Kim. S., and Lee. J., Lanthanide-Doped Upconversion Nanomaterials: Recent Advances and Applications, *BioChip J.*, **14**, 124–135 (2020).
16. Thygesen. K., Alpert. J. S., Jaffe. A. S., Chaitman. B. R., Bax. J. J., Morrow. D. A., White. H. D., and ESC Scientific Document Group, Fourth universal definition of myocardial infarction (2018), *Eur. Heart J.*, **40**, 237–269 (2019).
17. Wells. S. M. and Sleeper. M., Cardiac troponins, *J. Vet. Emerg. Crit. Care*, **18**, 235–245 (2008).
18. Mair. J., Lindahl. B., Hammarsten. O., Müller. C., Giannitsis. E., Huber. K., Möckel. M., Plebani. M., Thygesen. K., Jaffe. A. S., and on behalf of The European Society of Cardiology (ESC) Study Group on Biomarkers in Cardiology of the Acute Cardiovascular Care Association (ACCA), How is cardiac troponin released from injured myocardium?, *Eur. Heart J. Acute Cardiovasc. Care*, **7**, 553–560 (2018).
19. Collet. J.-P., Thiele. H., Barbato. E., Barthélémy. O., Bauersachs. J., Bhatt. D. L., Dendale. P., Dorobantu. M., Edvardsen. T., Folliguet. T., Gale. C. P., Gilard. M., Jobs. A., Jüni. P., Lambrinou. E., Lewis. B. S., Mehilli. J., Meliga. E., Merkely. B., Mueller. C., Roffi. M., Rutten. F. H., Sibbing. D., Siontis. G. C. M., Chettibi. M., Hayrapetyan. H. G., Metzler. B., Najafov. R., Stelmashok. V. I., Claeys. M., Kušljugić. Z., Gatzov. P. M., Skoric. B., Panayi. G., Mates. M., Sorensen. R., Shokry. K., Marandi. T., Kajander. O. A., Commeau. P., Aladashvili. A., Massberg. S., Nikas. D., Becker. D., Guðmundsdóttir. I. J., Peace. A. J., Beigel. R., Indolfi. C., Aidargaliyeva. N., Elezi. S., Beishenkulov. M., Maca. A., Gustiene. O., Degrell. P., Cassar Maempel. A., Ivanov. V., Damman. P., Kedev. S., Steigen. T. K., Legutko. J., Morais. J., Vinereanu. D., Duplyakov. D., Zavatta. M., Pavlović. M., Orban. M., Bunc. M., Ibañez. B., Hofmann. R., Gaemperli. O., Marjeh. Y. B., Addad. F., Tutar. E., Parkhomenko. A., Karia. N., and ESC Scientific Document Group, 2020 ESC Guidelines for the management of acute coronary syndromes in patients presenting without persistent ST-segment elevation: The Task Force for the management of acute coronary syndromes in patients presenting without persistent ST-segment elevation of the European Society of Cardiology (ESC), *Eur. Heart J.*, **42**, 1289–1367 (2021).
20. Wild. D., “Immunoassay for beginners”, In *The Immunoassay Handbook*, 4th Edn., Elsevier, 7–10 (n.d.).
21. EKINS. R. P., BASIC PRINCIPLES AND THEORY, *Br. Med. Bull.*, **30**, 3–11 (1974).
22. Pierson-Perry. J. F., EP17A2 | Evaluation of Detection Capability for Clinical Laboratory Measurement Procedures, 2nd Edition (2012).
23. Currie. L. A., Nomenclature in evaluation of analytical methods including detection and quantification capabilities (IUPAC Recommendations 1995), *Pure Appl. Chem.*, **67**, 1699–1723 (1995).
24. Ekins. R. P. and Chu. F. W., Multianalyte microspot immunoassay--microanalytical “compact disk” of the future, *Clin. Chem.*, **37**, 1955–1967 (1991).
25. Ekins. R. and Edwards. P., Point On the meaning of “sensitivity”, *Clin. Chem.*, **43**, 1824–1831 (1997).
26. Gorris. H. H. and Soukka. T., What Digital Immunoassays Can Learn from Ambient Analyte Theory: A Perspective, *Anal. Chem.*, **94**, 6073–6083 (2022).
27. Scatchard. G., The Attractions of Proteins for Small Molecules and Ions, *Ann. N. Y. Acad. Sci.*, **51**, 660–672 (1949).
28. Wild. D., *The Immunoassay Handbook - 4th Edition*, 4th Edn., Elsevier (2013).
29. Crothers. D. M. and Metzger. H., The influence of polyvalency on the binding properties of antibodies, *Immunochemistry*, **9**, 341–357 (1972).

30. Mammen. M., Choi. S.-K., and Whitesides. G. M., Polyvalent Interactions in Biological Systems: Implications for Design and Use of Multivalent Ligands and Inhibitors, *Angew. Chem. Int. Ed.*, **37**, 2754–2794 (1998).
31. Li. M.-H., Zong. H., Leroueil. P. R., Choi. S. K., and Baker. J. R. Jr., Ligand Characteristics Important to Avidity Interactions of Multivalent Nanoparticles, *Bioconjug. Chem.*, **28**, 1649–1657 (2017).
32. Soukka. T., Härmä. H., Paukkunen. J., and Lövgren. T., Utilization of Kinetically Enhanced Monovalent Binding Affinity by Immunoassays Based on Multivalent Nanoparticle-Antibody Bioconjugates, *Anal. Chem.*, **73**, 2254–2260 (2001).
33. Butler. J. E., Solid Supports in Enzyme-Linked Immunosorbent Assay and Other Solid-Phase Immunoassays, *Methods*, **22**, 4–23 (2000).
34. Sena-Torralba. A., Álvarez-Diduk. R., Parolo. C., Piper. A., and Merkoçi. A., Toward Next Generation Lateral Flow Assays: Integration of Nanomaterials, *Chem. Rev.*, **122**, 14881–14910 (2022).
35. "Architecture of a Lateral Flow Immunoassay", In *Lateral Flow Immunoassay*, Springer, New York, NY, 3–5 (2009).
36. "Unbacked nitrocellulose membranes", https://www.cytivalifesciences.com/en/kn/solutions/lab-filtration/knowledge-center/unbacked-membranes. Accessed02/2023.
37. Gubala. V., Harris. L. F., Ricco. A. J., Tan. M. X., and Williams. D. E., Point of Care Diagnostics: Status and Future, *Anal. Chem.*, **84**, 487–515 (2012).
38. Urdea. M., Penny. L. A., Olmsted. S. S., Giovanni. M. Y., Kaspar. P., Shepherd. A., Wilson. P., Dahl. C. A., Buchsbaum. S., Moeller. G., and Hay Burgess. D. C., Requirements for high impact diagnostics in the developing world, *Nature*, **444**, 73–79 (2006).
39. Mansfield. M. A., "Nitrocellulose Membranes for Lateral Flow Immunoassays: A Technical Treatise", In *Lateral Flow Immunoassay*, Springer, New York, NY, 95–113 (2009).
40. Merck Millipore, Rapid Lateral Flow Test Strips - Considerations for Product Development (2013).
41. Grant. B. D., Smith. C. A., Karvonen. K., and Richards-Kortum. R., Highly Sensitive Two-Dimensional Paper Network Incorporating Biotin–Streptavidin for the Detection of Malaria, *Anal. Chem.*, **88**, 2553–2557 (2016).
42. "Evolution in Lateral Flow–Based Immunoassay Systems", In *Lateral Flow Immunoassay*, Springer, New York, NY, 1–35 (2009).
43. Bishop. J. D., Hsieh. H. V., Gasperino. D. J., and Weigl. B. H., Sensitivity enhancement in lateral flow assays: a systems perspective, *Lab. Chip*, **19**, 2486–2499 (2019).
44. Lahtinen. S., Lyytikäinen. A., Sirkka. N., Päkkilä. H., and Soukka. T., Improving the sensitivity of immunoassays by reducing non-specific binding of poly(acrylic acid) coated upconverting nanoparticles by adding free poly(acrylic acid), *Microchim. Acta*, **185**, 220 (2018).
45. Lu. B., R. Smyth. M., and O'Kennedy. R., Tutorial review. Oriented immobilization of antibodies and its applications in immunoassays and immunosensors, *Analyst*, **121**, 29R-32R (1996).
46. Butler. J. E., Ni. L., Nessler. R., Joshi. K. S., Suter. M., Rosenberg. B., Chang. J., Brown. W. R., and Cantarero. L. A., The physical and functional behavior of capture antibodies adsorbed on polystyrene, *J. Immunol. Methods*, **150**, 77–90 (1992).
47. Davies. J., Dawkes. A. C., Haymes. A. G., Roberts. C. J., Sunderland. R. F., Wilkins. M. J., Davies. M. C., Tendler. S. J. B., Jackson. D. E., and Edwards. J. C., A scanning tunneling

microscopy comparison of passive antibody adsorption and biotinylated antibody linkage to streptavidin on microtiter wells, *J. Immunol. Methods*, **167**, 263–269 (1994).

48. Welch. N. G., Scoble. J. A., Muir. B. W., and Pigram. P. J., Orientation and characterization of immobilized antibodies for improved immunoassays (Review), *Biointerphases*, **12**, 02D301 (2017).
49. Schramm. W., Paek. S.-H., and Voss. G., Strategies for the Immobilization of Antibodies, *ImmunoMethods*, **3**, 93–103 (1993).
50. Jung. Y., Young Jeong. J., and Hyun Chung. B., Recent advances in immobilization methods of antibodies on solid supports, *Analyst*, **133**, 697–701 (2008).
51. Shen. M., Rusling. J. F., and Dixit. C. K., Site-selective orientated immobilization of antibodies and conjugates for immunodiagnostics development, *Methods*, **116**, 95–111 (2017).
52. Gao. S., Guisán. J. M., and Rocha-Martin. J., Oriented immobilization of antibodies onto sensing platforms - A critical review, *Anal. Chim. Acta*, **1189**, 338907 (2022).
53. Hermanson. G. T., *Bioconjugate Techniques*, Academic Press (2013).
54. Ylikotila. J., Välimaa. L., Takalo. H., and Pettersson. K., Improved surface stability and biotin binding properties of streptavidin coating on polystyrene, *Colloids Surf. B Biointerfaces*, **70**, 271–277 (2009).
55. Reznik. G. O., Vajda. S., Cantor. C. R., and Sano. T., A Streptavidin Mutant Useful for Directed Immobilization on Solid Surfaces, *Bioconjug. Chem.*, **12**, 1000–1004 (2001).
56. "Separation systems", In *The Immunoassay Handbook - 4th Edition*, 4th Edn., Elsevier, 287–299 (2013).
57. Low. S. C., Shaimi. R., Thandaithabany. Y., Lim. J. K., Ahmad. A. L., and Ismail. A., Electrophoretic interactions between nitrocellulose membranes and proteins: Biointerface analysis and protein adhesion properties, *Colloids Surf. B Biointerfaces*, **110**, 248–253 (2013).
58. Pelton. R., Bioactive paper provides a low-cost platform for diagnostics, *TrAC Trends Anal. Chem.*, **28**, 925–942 (2009).
59. de Puig. H., Bosch. I., Gehrke. L., and Hamad-Schifferli. K., Challenges of the nano-bio interface in lateral flow and dipstick immunoassays, *Trends Biotechnol.*, **35**, 1169–1180 (2017).
60. Ismail. A., Walker. P., Cawood. M., and Barth. J., Interference in immunoassay is an underestimated problem, *Ann. Clin. Biochem.*, **39**, 366–373 (2002).
61. Ward. G., Simpson. A., Boscato. L., and Hickman. P. E., The investigation of interferences in immunoassay, *Clin. Biochem.*, **50**, 1306–1311 (2017).
62. Tate. J. and Ward. G., Interferences in Immunoassay, *Clin. Biochem. Rev.*, **25**, 105–120 (2004).
63. Selby. C., Interference in Immunoassay, *Ann. Clin. Biochem.*, **36**, 704–721 (1999).
64. Kricka. L. J., Interferences in Immunoassay—Still a Threat, *Clin. Chem.*, **46**, 1037–1038 (2000).
65. Coutinho. A., Kazatchkine. M. D., and Avrameas. S., Natural autoantibodies, *Curr. Opin. Immunol.*, **7**, 812–818 (1995).
66. Eriksson. S., Halenius. H., Pulkki. K., Hellman. J., and Pettersson. K., Negative Interference in Cardiac Troponin I Immunoassays by Circulating Troponin Autoantibodies, *Clin. Chem.*, **51**, 839–847 (2005).
67. Kuusinen. S., Ekman. M., Raiko. K., Hannula. H., Lyytikäinen. A., Lahtinen. S., and Soukka. T., Complement C1q in plasma induces nonspecific binding of poly(acrylic acid)-coated upconverting nanoparticle antibody conjugates, *Anal. Bioanal. Chem.*, **414**, 3741–3749 (2022).

68. Wild. D., “Immunoassay performance measures”, In *The Immunoassay Handbook*, 4th Edn., Elsevier, 11–26 (n.d.).
69. Jin. B., Li. Z., Zhao. G., Ji. J., Chen. J., Yang. Y., and Xu. R., Upconversion fluorescence-based paper disc for multiplex point-of-care testing in water quality monitoring, *Anal. Chim. Acta*, **1192**, 339388 (2022).
70. Hecht. L., van Rossum. D., and Dietzel. A., Femtosecond-laser-structured nitrocellulose membranes for multi-parameter Point-of-Care tests, *Microelectron. Eng.*, **158**, 52–58 (2016).
71. Apilux. A., Ukita. Y., Chikae. M., Chailapakul. O., and Takamura. Y., Development of automated paper-based devices for sequential multistep sandwich enzyme-linked immunosorbent assays using inkjet printing, *Lab Chip*, **13**, 126–135 (2013).
72. Lu. Y., Shi. W., Qin. J., and Lin. B., Fabrication and Characterization of Paper-Based Microfluidics Prepared in Nitrocellulose Membrane By Wax Printing, *Anal. Chem.*, **82**, 329–335 (2010).
73. Carrilho. E., Martinez. A. W., and Whitesides. G. M., Understanding Wax Printing: A Simple Micropatterning Process for Paper-Based Microfluidics, *Anal. Chem.*, **81**, 7091–7095 (2009).
74. Rivas. L., Medina-Sánchez. M., de la Escosura-Muñiz. A., and Merkoçi. A., Improving sensitivity of gold nanoparticle-based lateral flow assays by using wax-printed pillars as delay barriers of microfluidics, *Lab Chip*, **14**, 4406–4414 (2014).
75. Lai. Y.-T., Tsai. C.-H., Hsu. J.-C., and Lu. Y.-W., Microfluidic Time-Delay Valve Mechanism on Paper-Based Devices for Automated Competitive ELISA, *Micromachines*, **10**, 837 (2019).
76. Chen. H., Cogswell. J., Anagnostopoulos. C., and Faghri. M., A fluidic diode, valves, and a sequential-loading circuit fabricated on layered paper, *Lab. Chip*, **12**, 2909 (2012).
77. Fu. E., Lutz. B., Kauffman. P., and Yager. P., Controlled reagent transport in disposable 2D paper networks, *Lab. Chip*, **10**, 918 (2010).
78. Alam. N., Tong. L., He. Z., Tang. R., Ahsan. L., and Ni. Y., Improving the sensitivity of cellulose fiber-based lateral flow assay by incorporating a water-dissolvable polyvinyl alcohol dam, *Cellulose*, **28**, 8641–8651 (2021).
79. Lutz. B., Liang. T., Fu. E., Ramachandran. S., Kauffman. P., and Yager. P., Dissolvable fluidic time delays for programming multi-step assays in instrument-free paper diagnostics, *Lab. Chip*, **13**, 2840 (2013).
80. Toley. B. J., McKenzie. B., Liang. T., Buser. J. R., Yager. P., and Fu. E., Tunable-Delay Shunts for Paper Microfluidic Devices, *Anal. Chem.*, **85**, 11545–11552 (2013).
81. Tang. R., Yang. H., Gong. Y., Liu. Z., Li. X., Wen. T., Qu. Z., Zhang. S., Mei. Q., and Xu. F., Improved Analytical Sensitivity of Lateral Flow Assay using Sponge for HBV Nucleic Acid Detection, *Sci. Rep.*, **7**, 1360 (2017).
82. Jiang. X. and Fan. Z. H., Fabrication and Operation of Paper-Based Analytical Devices, *Annu. Rev. Anal. Chem.*, **9**, 203–222 (2016).
83. Carrell. C., Kava. A., Nguyen. M., Menger. R., Munshi. Z., Call. Z., Nussbaum. M., and Henry. C., Beyond the lateral flow assay: A review of paper-based microfluidics, *Microelectron. Eng.*, **206**, 45–54 (2019).
84. Shen. M., Chen. Y., Zhu. Y., Zhao. M., and Xu. Y., Enhancing the Sensitivity of Lateral Flow Immunoassay by Centrifugation-Assisted Flow Control, *Anal. Chem.*, **91**, 4814–4820 (2019).
85. Shen. M., Li. N., Lu. Y., Cheng. J., and Xu. Y., An enhanced centrifugation-assisted lateral flow immunoassay for the point-of-care detection of protein biomarkers, *Lab. Chip*, **20**, 2626–2634 (2020).

86. Juntunen. E., Myyryläinen. T., Salminen. T., Soukka. T., and Pettersson. K., Performance of fluorescent europium(III) nanoparticles and colloidal gold reporters in lateral flow bioaffinity assay, *Anal. Biochem.*, **428**, 31–38 (2012).
87. Farka. Z., Mickert. M., Pastucha. M., Mikušová. Z., Skládal. P., and Gorris. H., Advances in optical single-molecule detection: On the road to super-sensitive bioaffinity assays, *Angew. Chem. Int. Ed.*, **59** (2019).
88. Danthanarayana. A. N., Brgoch. J., and Willson. R. C., Photoluminescent Molecules and Materials as Diagnostic Reporters in Lateral Flow Assays, *ACS Appl. Bio Mater.*, **5**, 82–96 (2022).
89. Ekins. R., Chu. F., and Micallef. J., High specific activity chemiluminescent and fluorescent markers: their potential application to high sensitivity and "multi-analyte" immunoassays, *J. Biolumin. Chemilumin.*, **4**, 59–78 (1989).
90. Yalow. R. S. and Berson. S. A., Assay of plasma insulin in human subjects by immunological methods, *Nature*, **184 (Suppl 21)**, 1648–1649 (1959).
91. Smith. D. S., Al-Hakiem. M. H. H., and Landon. J., A Review of Fluoroimmunoassay and Immunofluorometric Assay, *Ann. Clin. Biochem.*, **18**, 253–274 (1981).
92. Engvall. E. and Perlmann. P., Enzyme-linked immunosorbent assay (ELISA) quantitative assay of immunoglobulin G, *Immunochemistry*, **8**, 871–874 (1971).
93. Banala. S., Arts. R., Aper. S. J. A., and Merkx. M., No washing, less waiting: engineering biomolecular reporters for single-step antibody detection in solution, *Org. Biomol. Chem.*, **11**, 7642 (2013).
94. Hosseini. S., Vázquez-Villegas. P., Rito-Palomares. M., and Martinez-Chapa. S. O., "Step by Step with ELISA: Mechanism of Operation, Crucial Elements, Different Protocols, and Insights on Immobilization and Detection of Various Biomolecular Entities", In *Enzyme-Linked Immunosorbent Assay (ELISA): From A to Z*, S. Hosseini, P. Vázquez-Villegas, M. Rito-Palomares, and S. O. Martinez-Chapa, Eds., SpringerBriefs in Applied Sciences and Technology, Springer, Singapore, 31–56 (2018).
95. Medintz. I. L., Uyeda. H. T., Goldman. E. R., and Mattoussi. H., Quantum dot bioconjugates for imaging, labelling and sensing, *Nat. Mater.*, **4**, 435–446 (2005).
96. Takalo. H., Mukkala. V. M., Mikola. H., Liitti. P., and Hemmilä. I., Synthesis of europium(III) chelates suitable for labeling of bioactive molecules, *Bioconjug. Chem.*, **5**, 278–282 (1994).
97. Diaspro. A., Chirico. G., Usai. C., Ramoino. P., and Dobrucki. J., "Photobleaching", In *Handbook Of Biological Confocal Microscopy*, J. B. Pawley, Ed., Springer US, Boston, MA, 690–702 (2006).
98. Lisjak. D., Plohl. O., Ponikvar-Svet. M., and Majaron. B., Dissolution of upconverting fluoride nanoparticles in aqueous suspensions, *RSC Adv.*, **5**, 27393–27397 (2015).
99. Stokes. G. G., On the Change of Refrangibility of Light, *Philos. Trans. R. Soc. Lond.*, **142**, 463–562 (1852).
100. Lakowicz. J. R., Ed., "Introduction to Fluorescence", In *Principles of Fluorescence Spectroscopy*, Springer US, Boston, MA, 1–26 (2006).
101. Piruska. A., Nikcevic. I., Lee. S. H., Ahn. C., Heineman. W. R., Limbach. P. A., and Seliskar. C. J., The autofluorescence of plastic materials and chips measured under laser irradiation, *Lab. Chip*, **5**, 1348–1354 (2005).
102. Soini. E. and Hemmilä. I., Fluoroimmunoassay: present status and key problems., *Clin. Chem.*, **25**, 353–361 (1979).

103. Roth. S., Hadass. O., Cohen. M., Verbarg. J., Wilsey. J., and Danielli. A., Improving the Sensitivity of Fluorescence-Based Immunoassays by Photobleaching the Autofluorescence of Magnetic Beads, *Small Weinh. Bergstr. Ger.*, **15**, e1803751 (2019).
104. Zhang. K. Y., Yu. Q., Wei. H., Liu. S., Zhao. Q., and Huang. W., Long-Lived Emissive Probes for Time-Resolved Photoluminescence Bioimaging and Biosensing, *Chem. Rev.*, **118**, 1770–1839 (2018).
105. Connally. R. E. and Piper. J. A., Time-gated luminescence microscopy, *Ann. N. Y. Acad. Sci.*, **1130**, 106–116 (2008).
106. Urusov. A. E., Zherdev. A. V., and Dzantiev. B. B., Towards Lateral Flow Quantitative Assays: Detection Approaches, *Biosensors*, **9**, 89 (2019).
107. Danthanarayana. A. N., Finley. E., Vu. B., Kourentzi. K., Willson. R. C., and Brgoch. J., A multicolor multiplex lateral flow assay for high-sensitivity analyte detection using persistent luminescent nanophosphors, *Anal. Methods Adv. Methods Appl.*, **12**, 272–280 (2020).
108. Lee. L. G., Nordman. E. S., Johnson. M. D., and Oldham. M. F., A Low-Cost, High-Performance System for Fluorescence Lateral Flow Assays, *Biosensors*, **3**, 360–373 (2013).
109. Juntunen. E., "Lateral flow immunoassays with fluorescent reporter technologies", (2018).
110. Faulstich. K., Gruler. R., Eberhard. M., Lentzsch. D., and Haberstroh. K., "Handheld and Portable Reader Devices for Lateral Flow Immunoassays", In *Lateral Flow Immunoassay*, R. Wong and H. Tse, Eds., Humana Press, Totowa, NJ, 1–27 (2009).
111. Pham. A. T. T., Wallace. A., Zhang. X., Tohl. D., Fu. H., Chuah. C., Reynolds. K. J., Ramsey. C., and Tang. Y., Optical-Based Biosensors and Their Portable Healthcare Devices for Detecting and Monitoring Biomarkers in Body Fluids, *Diagnostics*, **11**, 1285 (2021).
112. Farka. Z., Mickert. M. J., Pastucha. M., Mikušová. Z., Skládal. P., and Gorris. H. H., Advances in Optical Single-Molecule Detection: En Route to Supersensitive Bioaffinity Assays, *Angew. Chem. Int. Ed.*, **59**, 10746–10773 (2020).
113. Ekins. R. P., Ligand assays: from electrophoresis to miniaturized microarrays, *Clin. Chem.*, **44**, 2015–2030 (1998).
114. Walt. D. R., Optical Methods for Single Molecule Detection and Analysis, *Anal. Chem.*, **85**, 1258–1263 (2013).
115. Hasinoff. S. W., "Photon, Poisson Noise", In *Computer Vision: A Reference Guide*, K. Ikeuchi, Ed., Springer US, Boston, MA, 608–610 (2014).
116. Loo. J. F.-C., Chien. Y.-H., Yin. F., Kong. S.-K., Ho. H.-P., and Yong. K.-T., Upconversion and downconversion nanoparticles for biophotonics and nanomedicine, *Coord. Chem. Rev.*, **400**, 213042 (2019).
117. Auzel. F., Spectral narrowing of excitation spectra in n-photons up-conversion processes by energy transfers, *J. Lumin.*, **31–32**, 759–761 (1984).
118. Mansfield. J. R., Gossage. K. W., Hoyt. C. C., and M.d. R. M. L., Autofluorescence removal, multiplexing, and automated analysis methods for in-vivo fluorescence imaging, *J. Biomed. Opt.*, **10**, 041207 (2005).
119. Soukka. T., Kuningas. K., Rantanen. T., Haaslahti. V., and Lövgren. T., Photochemical Characterization of Up-Converting Inorganic Lanthanide Phosphors as Potential Labels, *J. Fluoresc.*, **15**, 513–528 (2005).
120. Nadort. A., Zhao. J., and Goldys. E. M., Lanthanide upconversion luminescence at the nanoscale: fundamentals and optical properties, *Nanoscale*, **8**, 13099–13130 (2016).
121. Chen. J. and Zhao. J. X., Upconversion Nanomaterials: Synthesis, Mechanism, and Applications in Sensing, *Sensors*, **12**, 2414–2435 (2012).

122. Suyver. J. F., Aebischer. A., Biner. D., Gerner. P., Grimm. J., Heer. S., Krämer. K. W., Reinhard. C., and Güdel. H. U., Novel materials doped with trivalent lanthanides and transition metal ions showing near-infrared to visible photon upconversion, *Opt. Mater.*, **27**, 1111–1130 (2005).
123. Auzel. F., Upconversion processes in coupled ion systems, *J. Lumin.*, **45**, 341–345 (1990).
124. Wang. Y., Tu. L., Zhao. J., Sun. Y., Kong. X., and Zhang. H., Upconversion Luminescence of β-NaYF4: Yb3+, Er3+@β-NaYF4 Core/Shell Nanoparticles: Excitation Power Density and Surface Dependence, *J. Phys. Chem. C*, **113**, 7164–7169 (2009).
125. Pollnau. M., Gamelin. D. R., Lüthi. S. R., Güdel. H. U., and Hehlen. M. P., Power dependence of upconversion luminescence in lanthanide and transition-metal-ion systems, *Phys. Rev. B*, **61**, 3337–3346 (2000).
126. Joseph. R. E., Jiménez. C., Hudry. D., Gao. G., Busko. D., Biner. D., Turshatov. A., Krämer. K., Richards. B. S., and Howard. I. A., Critical Power Density: A Metric To Compare the Excitation Power Density Dependence of Photon Upconversion in Different Inorganic Host Materials, *J. Phys. Chem. A*, **123**, 6799–6811 (2019).
127. Joseph. R. E., Busko. D., Hudry. D., Gao. G., Biner. D., Krämer. K., Turshatov. A., Richards. B. S., and Howard. I. A., A method for correcting the excitation power density dependence of upconversion emission due to laser-induced heating, *Opt. Mater.*, **82**, 65–70 (2018).
128. Menyuk. N., Dwight. K., and Pierce. J. w., NaYF4 : Yb,Er—an efficient upconversion phosphor, *Appl. Phys. Lett.*, **21**, 159–161 (1972).
129. Jung. T., Jo. H. L., Nam. S. H., Yoo. B., Cho. Y., Kim. J., Kim. H. M., Hyeon. T., Suh. Y. D., Lee. H., and Lee. K. T., The preferred upconversion pathway for the red emission of lanthanide-doped upconverting nanoparticles, NaYF4:Yb3+,Er3+, *Phys. Chem. Chem. Phys.*, **17**, 13201–13205 (2015).
130. Shin. K., Jung. T., Lee. E., Lee. G., Goh. Y., Heo. J., Jung. M., Jo. E.-J., Lee. H., Kim. M.-G., and Lee. K. T., Distinct mechanisms for the upconversion of NaYF4:Yb3+,Er3+ nanoparticles revealed by stimulated emission depletion, *Phys. Chem. Chem. Phys.*, **19**, 9739–9744 (2017).
131. Anderson. R., Smith. S., May. S., and Mary. B., Revisiting the NIR-to-Visible Upconversion Mechanism in beta-NaYF4:Yb3+,Er3+, *J. Phys. Chem. Lett.*, **5**, 36–42 (2013).
132. Berry. M. T. and May. P. S., Disputed Mechanism for NIR-to-Red Upconversion Luminescence in NaYF4:Yb3+,Er3+, *J. Phys. Chem. A*, **119**, 9805–9811 (2015).
133. Wilhelm. S., Kaiser. M., Würth. C., Heiland. J., Carrillo-Carrion. C., Muhr. V., Wolfbeis. O. S., Parak. W. J., Resch-Genger. U., and Hirsch. T., Water dispersible upconverting nanoparticles: effects of surface modification on their luminescence and colloidal stability, *Nanoscale*, **7**, 1403–1410 (2015).
134. Cong. T., Ding. Y., Xin. S., Hong. X., Zhang. H., and Liu. Y., Solvent-Induced Luminescence Variation of Upconversion Nanoparticles, *Langmuir*, **32**, 13200–13206 (2016).
135. Boyer. J.-C., Manseau. M.-P., Murray. J. I., and van Veggel. F. C. J. M., Surface Modification of Upconverting NaYF4 Nanoparticles with PEG−Phosphate Ligands for NIR (800 nm) Biolabeling within the Biological Window, *Langmuir*, **26**, 1157–1164 (2010).
136. Hyppänen. I., Höysniemi. N., Arppe. R., Schäferling. M., and Soukka. T., Environmental Impact on the Excitation Path of the Red Upconversion Emission of Nanocrystalline NaYF4:Yb3+,Er3+, *J. Phys. Chem. C*, **121**, 6924–6929 (2017).
137. Würth. C., Kaiser. M., Wilhelm. S., Grauel. B., Hirsch. T., and Resch-Genger. U., Excitation power dependent population pathways and absolute quantum yields of upconversion nanoparticles in different solvents, *Nanoscale*, **9**, 4283–4294 (2017).

138. Lahtinen. S., Upconverting nanoparticles in bioaffinity assays : new insights and perspectives (2019).
139. Wang. F., Han. Y., Lim. C. S., Lu. Y., Wang. J., Xu. J., Chen. H., Zhang. C., Hong. M., and Liu. X., Simultaneous phase and size control of upconversion nanocrystals through lanthanide doping, *Nature*, **463**, 1061–1065 (2010).
140. Sedlmeier. A., Achatz. D. E., Fischer. L. H., Gorris. H. H., and Wolfbeis. O. S., Photon upconverting nanoparticles for luminescent sensing of temperature, *Nanoscale*, **4**, 7090–7096 (2012).
141. Xiang. G., Zhang. J., Hao. Z., Zhang. X., Pan. G.-H., Luo. Y., Lü. W., and Zhao. H., Importance of suppression of Yb(3+) de-excitation to upconversion enhancement in β-NaYF4: Yb(3+)/Er(3+)@β-NaYF4 sandwiched structure nanocrystals, *Inorg. Chem.*, **54**, 3921–3928 (2015).
142. Fischer. S., Bronstein. N. D., Swabeck. J. K., Chan. E. M., and Alivisatos. A. P., Precise Tuning of Surface Quenching for Luminescence Enhancement in Core–Shell Lanthanide-Doped Nanocrystals, *Nano Lett.*, **16**, 7241–7247 (2016).
143. Gorris. H. H. and Wolfbeis. O. S., Photon-Upconverting Nanoparticles for Optical Encoding and Multiplexing of Cells, Biomolecules, and Microspheres, *Angew. Chem. Int. Ed.*, **52**, 3584–3600 (2013).
144. Dong. H., Sun. L.-D., and Yan. C.-H., Energy transfer in lanthanide upconversion studies for extended optical applications, *Chem. Soc. Rev.*, **44**, 1608–1634 (2015).
145. Soukka. T. and Härmä. H., Eds., "Lanthanide Nanoparticules as Photoluminescent Reporters", In *Lanthanide Luminescence: Photophysical, Analytical and Biological Aspects*, Springer Series on Fluorescence, Springer Berlin Heidelberg, Berlin, Heidelberg, **7**, 89–113 (2011).
146. Lee. S., Lee. J., Cao. Y., An. C., and Kang. S. H., Nanomaterial-based single-molecule optical immunosensors for supersensitive detection, *Biosens. Bioelectron. X*, **11**, 100191 (2022).
147. Mickert. M. J., Farka. Z., Kostiv. U., Hlaváček. A., Horák. D., Skládal. P., and Gorris. H. H., Measurement of Sub-femtomolar Concentrations of Prostate-Specific Antigen through Single-Molecule Counting with an Upconversion-Linked Immunosorbent Assay, *Anal. Chem.*, **91**, 9435–9441 (2019).
148. Brandmeier. J. C., Jurga. N., Grzyb. T., Hlaváček. A., Obořilová. R., Skládal. P., Farka. Z., and Gorris. H. H., Digital and Analog Detection of SARS-CoV-2 Nucleocapsid Protein via an Upconversion-Linked Immunosorbent Assay, *Anal. Chem.* (2023).
149. Kraft. M., Würth. C., Muhr. V., Hirsch. T., and Resch-Genger. U., Particle-size-dependent upconversion luminescence of NaYF4: Yb, Er nanoparticles in organic solvents and water at different excitation power densities, *Nano Res.*, **11**, 6360–6374 (2018).
150. Quintanilla. M., Cantarelli. I. X., Pedroni. M., Speghini. A., and Vetrone. F., Intense ultraviolet upconversion in water dispersible SrF2:Tm3+,Yb3+ nanoparticles: the effect of the environment on light emissions, *J. Mater. Chem. C*, **3**, 3108–3113 (2015).
151. Wang. Y.-F., Sun. L.-D., Xiao. J.-W., Feng. W., Zhou. J.-C., Shen. J., and Yan. C.-H., Rare-Earth Nanoparticles with Enhanced Upconversion Emission and Suppressed Rare-Earth-Ion Leakage, *Chem. – Eur. J.*, **18**, 5558–5564 (2012).
152. Lahtinen. S., Lyytikäinen. A., Päkkilä. H., Hömppi. E., Perälä. N., Lastusaari. M., and Soukka. T., Disintegration of Hexagonal NaYF4:Yb3+,Er3+ Upconverting Nanoparticles in Aqueous Media: The Role of Fluoride in Solubility Equilibrium, *J. Phys. Chem. C*, **121**, 656–665 (2017).
153. Plohl. O., Kraft. M., Kovač. J., Belec. B., Ponikvar-Svet. M., Würth. C., Lisjak. D., and Resch-Genger. U., Optically Detected Degradation of NaYF4:Yb,Tm-Based Upconversion Nanoparticles in Phosphate Buffered Saline Solution, *Langmuir*, **33**, 553–560 (2017).

154. Hlaváček. A., Mickert. M. J., Soukka. T., Lahtinen. S., Tallgren. T., Pizúrová. N., Król. A., and Gorris. H. H., Large-Scale Purification of Photon-Upconversion Nanoparticles by Gel Electrophoresis for Analogue and Digital Bioassays, *Anal. Chem.*, **91**, 1241–1246 (2019).
155. Farka. Z., Mickert. M. J., Hlaváček. A., Skládal. P., and Gorris. H. H., Single Molecule Upconversion-Linked Immunosorbent Assay with Extended Dynamic Range for the Sensitive Detection of Diagnostic Biomarkers, *Anal. Chem.*, **89**, 11825–11830 (2017).
156. Mader. H. S., Kele. P., Saleh. S. M., and Wolfbeis. O. S., Upconverting luminescent nanoparticles for use in bioconjugation and bioimaging, *Curr. Opin. Chem. Biol.*, **14**, 582–596 (2010).
157. Lahtinen. S., Baldtzer Liisberg. M., Raiko. K., Krause. S., Soukka. T., and Vosch. T., Thulium- and Erbium-Doped Nanoparticles with Poly(acrylic acid) Coating for Upconversion Cross-Correlation Spectroscopy-based Sandwich Immunoassays in Plasma, *ACS Appl. Nano Mater.*, **4**, 432–440 (2021).
158. Kong. W., Sun. T., Chen. B., Chen. X., Ai. F., Zhu. X., Li. M., Zhang. W., Zhu. G., and Wang. F., A General Strategy for Ligand Exchange on Upconversion Nanoparticles, *Inorg. Chem.*, **56**, 872–877 (2017).
159. Zhu. X., Zhang. H., and Zhang. F., Ligand-Based Surface Engineering of Lanthanide Nanoparticles for Bioapplications, *ACS Mater. Lett.*, **4**, 1815–1830 (2022).
160. Shiby. E., Reddy. K. L., and Kumar. J., A Facile Approach for the Ligand Free Synthesis of Biocompatible Upconversion Nanophosphors, *Front. Chem.*, **10**, 904676 (2022).
161. Bogdan. N., Vetrone. F., Ozin. G. A., and Capobianco. J. A., Synthesis of Ligand-Free Colloidally Stable Water Dispersible Brightly Luminescent Lanthanide-Doped Upconverting Nanoparticles, *Nano Lett.*, **11**, 835–840 (2011).
162. Yüce. M. and Kurt. H., How to make nanobiosensors: surface modification and characterisation of nanomaterials for biosensing applications, *RSC Adv.*, **7**, 49386–49403 (2017).
163. Lingeshwar Reddy. K., Srinivas. V., Shankar. K. R., Kumar. S., Sharma. V., Kumar. A., Bahuguna. A., Bhattacharyya. K., and Krishnan. V., Enhancement of Luminescence Intensity in Red Emitting NaYF4:Yb/Ho/Mn Upconversion Nanophosphors by Variation of Reaction Parameters, *J. Phys. Chem. C*, **121**, 11783–11793 (2017).
164. Muhr. V., Würth. C., Kraft. M., Buchner. M., Baeumner. A. J., Resch-Genger. U., and Hirsch. T., Particle-Size-Dependent Förster Resonance Energy Transfer from Upconversion Nanoparticles to Organic Dyes, *Anal. Chem.*, **89**, 4868–4874 (2017).
165. Guo. Q., Liu. Y., Jia. Q., Zhang. G., Fan. H., Liu. L., and Zhou. J., Ultrahigh Sensitivity Multifunctional Nanoprobe for the Detection of Hydroxyl Radical and Evaluation of Heavy Metal Induced Oxidative Stress in Live Hepatocyte, *Anal. Chem.*, **89**, 4986–4993 (2017).
166. Yi. G.-S. and Chow. G.-M., Water-Soluble NaYF4:Yb,Er(Tm)/NaYF4/Polymer Core/Shell/Shell Nanoparticles with Significant Enhancement of Upconversion Fluorescence, *Chem. Mater.*, **19**, 341–343 (2007).
167. Li. L.-L., Zhang. R., Yin. L., Zheng. K., Qin. W., Selvin. P. R., and Lu. Y., Biomimetic Surface Engineering of Lanthanide-Doped Upconversion Nanoparticles as Versatile Bioprobes, *Angew. Chem. Int. Ed.*, **51**, 6121–6125 (2012).
168. Lin. C.-A. J., Sperling. R. A., Li. J. K., Yang. T.-Y., Li. P.-Y., Zanella. M., Chang. W. H., and Parak. W. J., Design of an Amphiphilic Polymer for Nanoparticle Coating and Functionalization, *Small*, **4**, 334–341 (2008).

169. Jiang. W., Mardyani. S., Fischer. H., and Chan. W. C. W., Design and Characterization of Lysine Cross-Linked Mercapto-Acid Biocompatible Quantum Dots, *Chem. Mater.*, **18**, 872–878 (2006).
170. Pellegrino. T., Manna. L., Kudera. S., Liedl. T., Koktysh. D., Rogach. A. L., Keller. S., Rädler. J., Natile. G., and Parak. W. J., Hydrophobic Nanocrystals Coated with an Amphiphilic Polymer Shell: A General Route to Water Soluble Nanocrystals, *Nano Lett.*, **4**, 703–707 (2004).
171. Kang. Y. and Taton. T. A., Core/Shell Gold Nanoparticles by Self-Assembly and Crosslinking of Micellar, Block-Copolymer Shells, *Angew. Chem. Int. Ed.*, **44**, 409–412 (2005).
172. Abdul Jalil. R. and Zhang. Y., Biocompatibility of silica coated NaYF4 upconversion fluorescent nanocrystals, *Biomaterials*, **29**, 4122–4128 (2008).
173. Zhang. Q., Song. K., Zhao. J., Kong. X., Sun. Y., Liu. X., Zhang. Y., Zeng. Q., and Zhang. H., Hexanedioic acid mediated surface-ligand-exchange process for transferring NaYF4:Yb/Er (or Yb/Tm) up-converting nanoparticles from hydrophobic to hydrophilic, *J. Colloid Interface Sci.*, **336**, 171–175 (2009).
174. Himmelstoß. S. F. and Hirsch. T., Long-Term Colloidal and Chemical Stability in Aqueous Media of NaYF4-Type Upconversion Nanoparticles Modified by Ligand-Exchange, *Part. Part. Syst. Charact.*, **36**, 1900235 (2019).
175. Naccache. R., Chevallier. P., Lagueux. J., Gossuin. Y., Laurent. S., Vander Elst. L., Chilian. C., Capobianco. J. A., and Fortin. M.-A., High Relaxivities and Strong Vascular Signal Enhancement for NaGdF4 Nanoparticles Designed for Dual MR/Optical Imaging, *Adv. Healthc. Mater.*, **2**, 1478–1488 (2013).
176. Arnett. L. P., Liu. J., Zhang. Y., Cho. H., Lu. E., Closson. T., Allo. B., and Winnik. M. A., Biotinylated Lipid-Coated NaLnF $_4$ Nanoparticles: Demonstrating the Use of Lanthanide Nanoparticle-Based Reporters in Suspension and Imaging Mass Cytometry, *Langmuir*, **38**, 2525–2537 (2022).
177. Pichaandi. J., Tong. L., Bouzekri. A., Yu. Q., Ornatsky. O., Baranov. V., and Winnik. M. A., Liposome-Encapsulated NaLnF4 Nanoparticles for Mass Cytometry: Evaluating Nonspecific Binding to Cells, *Chem. Mater.*, **29**, 4980–4990 (2017).
178. Wang. F., Deng. R., Wang. J., Wang. Q., Han. Y., Zhu. H., Chen. X., and Liu. X., Tuning upconversion through energy migration in core–shell nanoparticles, *Nat. Mater.*, **10**, 968–973 (2011).
179. Tsuda. A. and Venkata. N. K., The role of natural processes and surface energy of inhaled engineered nanoparticles on aggregation and corona formation, *NanoImpact*, **2**, 38–44 (2016).
180. Klimkevicius. V., Voronovic. E., Jarockyte. G., Skripka. A., Vetrone. F., Rotomskis. R., Katelnikovas. A., and Karabanovas. V., Polymer brush coated upconverting nanoparticles with improved colloidal stability and cellular labeling, *J. Mater. Chem. B*, **10**, 625–636 (2022).
181. Dong. A., Ye. X., Chen. J., Kang. Y., Gordon. T., Kikkawa. J. M., and Murray. C. B., A Generalized Ligand-Exchange Strategy Enabling Sequential Surface Functionalization of Colloidal Nanocrystals, *J. Am. Chem. Soc.*, **133**, 998–1006 (2011).
182. Estebanez. N., González-Béjar. M., and Pérez-Prieto. J., Polysulfonate Cappings on Upconversion Nanoparticles Prevent Their Disintegration in Water and Provide Superior Stability in a Highly Acidic Medium, *ACS Omega*, **4**, 3012–3019 (2019).
183. Sirkka. N., Lyytikäinen. A., Savukoski. T., and Soukka. T., Upconverting nanophosphors as reporters in a highly sensitive heterogeneous immunoassay for cardiac troponin I, *Anal. Chim. Acta*, **925**, 82–87 (2016).

184. Ukonaho. T., Rantanen. T., Jämsen. L., Kuningas. K., Päkkilä. H., Lövgren. T., and Soukka. T., Comparison of infrared-excited up-converting phosphors and europium nanoparticles as labels in a two-site immunoassay, *Anal. Chim. Acta*, **596**, 106–115 (2007).
185. Liang. L., Everest-Dass. A. V., Kostyuk. A. B., Khabir. Z., Zhang. R., Trushina. D. B., and Zvyagin. A. V., The Surface Charge of Polymer-Coated Upconversion Nanoparticles Determines Protein Corona Properties and Cell Recognition in Serum Solutions, *Cells*, **11**, 3644 (2022).
186. Zijlmans. H. J. M. A. A., Bonnet. J., Burton. J., Kardos. K., Vail. T., Niedbala. R. S., and Tanke. H. J., Detection of Cell and Tissue Surface Antigens Using Up-Converting Phosphors: A New Reporter Technology, *Anal. Biochem.*, **267**, 30–36 (1999).
187. Shapoval. O., Brandmeier. J. C., Nahorniak. M., Oleksa. V., Makhneva. E., Gorris. H. H., Farka. Z., and Horák. D., PMVEMA-coated upconverting nanoparticles for upconversion-linked immunoassay of cardiac troponin, *Talanta*, **244**, 123400 (2022).
188. Pastucha. M., Odstrčilíková. E., Hlaváček. A., Brandmeier. J. C., Vykoukal. V., Weisová. J., Gorris. H. H., Skládal. P., and Farka. Z., Upconversion-Linked Immunoassay for the Diagnosis of Honeybee Disease American Foulbrood, *IEEE J. Sel. Top. Quantum Electron.*, **27**, 1–11 (2021).
189. Zhou. C., Chu. Z., Hou. W., and Wang. X., Lanthanide-Doped Upconversion-Linked Immunosorbent Assay for the Sensitive Detection of Carbohydrate Antigen 19-9, *Front. Chem.*, **8** (2021).
190. Poláchová. V., Pastucha. M., Mikušová. Z., Mickert. M. J., Hlaváček. A., Gorris. H. H., Skládal. P., and Farka. Z., Click-conjugated photon-upconversion nanoparticles in an immunoassay for honeybee pathogen Melissococcus plutonius, *Nanoscale*, **11**, 8343–8351 (2019).
191. Hlaváček. A., Peterek. M., Farka. Z., Mickert. M. J., Prechtl. L., Knopp. D., and Gorris. H. H., Rapid single-step upconversion-linked immunosorbent assay for diclofenac, *Microchim. Acta*, **184**, 4159–4165 (2017).
192. Juntunen. E., Salminen. T., Talha. S. M., Martiskainen. I., Soukka. T., Pettersson. K., and Waris. M., Lateral flow immunoassay with upconverting nanoparticle-based detection for indirect measurement of interferon response by the level of MxA, *J. Med. Virol.*, **89**, 598–605 (2017).
193. Martiskainen. I., Talha. S. M., Vuorenpää. K., Salminen. T., Juntunen. E., Chattopadhyay. S., Kumar. D., Vuorinen. T., Pettersson. K., Khanna. N., and Batra. G., Upconverting nanoparticle reporter–based highly sensitive rapid lateral flow immunoassay for hepatitis B virus surface antigen, *Anal. Bioanal. Chem.*, **413**, 967–978 (2021).
194. Salminen. T., Mehdi. F., Rohila. D., Kumar. M., Talha. S. M., Prakash. J. A. J., Khanna. N., Pettersson. K., and Batra. G., Ultrasensitive and Robust Point-of-Care Immunoassay for the Detection of Plasmodium falciparum Malaria, *Anal. Chem.*, **92**, 15766–15772 (2020).
195. Gong. Y., Zheng. Y., Jin. B., You. M., Wang. J., Li. X., Lin. M., Xu. F., and Li. F., A portable and universal upconversion nanoparticle-based lateral flow assay platform for point-of-care testing, *Talanta*, **201**, 126–133 (2019).
196. He. M., Li. Z., Ge. Y., and Liu. Z., Portable Upconversion Nanoparticles-Based Paper Device for Field Testing of Drug Abuse, *Anal. Chem.*, **88**, 1530–1534 (2016).
197. Giust. D., Lucío. M. I., El-Sagheer. A. H., Brown. T., Williams. L. E., Muskens. O. L., and Kanaras. A. G., Graphene Oxide–Upconversion Nanoparticle Based Portable Sensors for Assessing Nutritional Deficiencies in Crops, *ACS Nano*, **12**, 6273–6279 (2018).

198. You. M., Lin. M., Gong. Y., Wang. S., Li. A., Ji. L., Zhao. H., Ling. K., Wen. T., Huang. Y., Gao. D., Ma. Q., Wang. T., Ma. A., Li. X., and Xu. F., Household Fluorescent Lateral Flow Strip Platform for Sensitive and Quantitative Prognosis of Heart Failure Using Dual-Color Upconversion Nanoparticles, *ACS Nano*, **11**, 6261–6270 (2017).
199. Hu. X., Wei. T., Wang. J., Liu. Z.-E., Li. X., Zhang. B., Li. Z., Li. L., and Yuan. Q., Near-Infrared-Light Mediated Ratiometric Luminescent Sensor for Multimode Visualized Assays of Explosives, *Anal. Chem.*, **86**, 10484–10491 (2014).
200. Yan. Z., Zhou. L., Zhao. Y., Wang. J., Huang. L., Hu. K., Liu. H., Wang. H., Guo. Z., Song. Y., Huang. H., and Yang. R., Rapid quantitative detection of Yersinia pestis by lateral-flow immunoassay and up-converting phosphor technology-based biosensor, *Sens. Actuators B Chem.*, **119**, 656–663 (2006).
201. Kozel. T. R. and Burnham-Marusich. A. R., Point-of-Care Testing for Infectious Diseases: Past, Present, and Future, *J. Clin. Microbiol.*, **55**, 2313–2320 (2017).
202. Yang. X., Liu. L., Hao. Q., Zou. D., Zhang. X., Zhang. L., Li. H., Qiao. Y., Zhao. H., and Zhou. L., Development and Evaluation of Up-Converting Phosphor Technology-Based Lateral Flow Assay for Quantitative Detection of NT-proBNP in Blood, *PLoS ONE*, **12**, e0171376 (2017).
203. Ji. T., Xu. X., Wang. X., Zhou. Q., Ding. W., Chen. B., Guo. X., Hao. Y., and Chen. G., Point of care upconversion nanoparticles-based lateral flow assay quantifying myoglobin in clinical human blood samples, *Sens. Actuators B Chem.*, **282**, 309–316 (2019).
204. Bayoumy. S., Martiskainen. I., Heikkilä. T., Rautanen. C., Hedberg. P., Hyytiä. H., Wittfooth. S., and Pettersson. K., Sensitive and quantitative detection of cardiac troponin I with upconverting nanoparticle lateral flow test with minimized interference, *Sci. Rep.*, **11**, 18698 (2021).
205. Liu. C., Qiu. X., Ongagna. S., Chen. D., Chen. Z., Abrams. W. R., Malamud. D., Corstjens. P. L. A. M., and Bau. H. H., A timer-actuated immunoassay cassette for detecting molecular markers in oral fluids, *Lab Chip*, **9**, 768–776 (2009).
206. Thygesen. K., Mair. J., Katus. H., Plebani. M., Venge. P., Collinson. P., Lindahl. B., Giannitsis. E., Hasin. Y., Galvani. M., Tubaro. M., Alpert. J. S., Biasucci. L. M., Koenig. W., Mueller. C., Huber. K., Hamm. C., Jaffe. A. S., and the Study Group on Biomarkers in Cardiology of the ESC Working Group on Acute Cardiac Care, Recommendations for the use of cardiac troponin measurement in acute cardiac care†, *Eur. Heart J.*, **31**, 2197–2204 (2010).
207. Katrukha. I. A., Human cardiac troponin complex. Structure and functions, *Biochem. Biokhimiia*, **78**, 1447–1465 (2013).
208. Rittoo. D., Jones. A., Lecky. B., and Neithercut. D., Elevation of Cardiac Troponin T, But Not Cardiac Troponin I, in Patients With Neuromuscular Diseases: Implications for the Diagnosis of Myocardial Infarction, *J. Am. Coll. Cardiol.*, **63**, 2411–2420 (2014).
209. Jaffe. A. S., Vasile. V. C., Milone. M., Saenger. A. K., Olson. K. N., and Apple. F. S., Diseased Skeletal Muscle: A Noncardiac Source of Increased Circulating Concentrations of Cardiac Troponin T, *J. Am. Coll. Cardiol.*, **58**, 1819–1824 (2011).
210. Wens. S. C. A., Schaaf. G. J., Michels. M., Kruijshaar. M. E., van Gestel. T. J. M., in 't Groen. S., Pijnenburg. J., Dekkers. D. H. W., Demmers. J. A. A., Verdijk. L. B., Brusse. E., van Schaik. R. H. N., van der Ploeg. A. T., van Doorn. P. A., and Pijnappel. W. W. M. P., Elevated Plasma Cardiac Troponin T Levels Caused by Skeletal Muscle Damage in Pompe Disease, *Circ. Cardiovasc. Genet.*, **9**, 6–13 (2016).

211. Mair. J., Lindahl. B., Müller. C., Giannitsis. E., Huber. K., Möckel. M., Plebani. M., Thygesen. K., and Jaffe. A. S., What to do when you question cardiac troponin values, *Eur. Heart J. Acute Cardiovasc. Care*, **7**, 577–586 (2018).
212. Unger. E. D., Dubin. R. F., Deo. R., Daruwalla. V., Friedman. J. L., Medina. C., Beussink. L., Freed. B. H., and Shah. S. J., Association of chronic kidney disease with abnormal cardiac mechanics and adverse outcomes in patients with heart failure and preserved ejection fraction, *Eur. J. Heart Fail.*, **18**, 103–112 (2016).
213. Twerenbold. R., Wildi. K., Jaeger. C., Gimenez. M. R., Reiter. M., Reichlin. T., Walukiewicz. A., Gugala. M., Krivoshei. L., Marti. N., Moreno Weidmann. Z., Hillinger. P., Puelacher. C., Rentsch. K., Honegger. U., Schumacher. C., Zurbriggen. F., Freese. M., Stelzig. C., Campodarve. I., Bassetti. S., Osswald. S., and Mueller. C., Optimal Cutoff Levels of More Sensitive Cardiac Troponin Assays for the Early Diagnosis of Myocardial Infarction in Patients With Renal Dysfunction, *Circulation*, **131**, 2041–2050 (2015).
214. deFilippi. C., Seliger. S. L., Kelley. W., Duh. S.-H., Hise. M., Christenson. R. H., Wolf. M., Gaggin. H., and Januzzi. J., Interpreting cardiac troponin results from high-sensitivity assays in chronic kidney disease without acute coronary syndrome, *Clin. Chem.*, **58**, 1342–1351 (2012).
215. Weil. B. R., Suzuki. G., Young. R. F., Iyer. V., and Canty. J. M., Troponin Release and Reversible Left Ventricular Dysfunction After Transient Pressure Overload, *J. Am. Coll. Cardiol.*, **71**, 2906–2916 (2018).
216. Goodman. S. G., Steg. P. G., Eagle. K. A., Fox. K. A. A., López-Sendón. J., Montalescot. G., Budaj. A., Kennelly. B. M., Gore. J. M., Allegrone. J., Granger. C. B., and Gurfinkel. E. P., The diagnostic and prognostic impact of the redefinition of acute myocardial infarction: Lessons from the Global Registry of Acute Coronary Events (GRACE), *Am. Heart J.*, **151**, 654–660 (2006).
217. Reichlin. T., Irfan. A., Twerenbold. R., Reiter. M., Hochholzer. W., Burkhalter. H., Bassetti. S., Steuer. S., Winkler. K., Peter. F., Meissner. J., Haaf. P., Potocki. M., Drexler. B., Osswald. S., and Mueller. C., Utility of Absolute and Relative Changes in Cardiac Troponin Concentrations in the Early Diagnosis of Acute Myocardial Infarction, *Circulation*, **124**, 136–145 (2011).
218. Apple. F. S., Collinson. P. O., and for the IFCC Task Force on Clinical Applications of Cardiac Biomarkers, Analytical Characteristics of High-Sensitivity Cardiac Troponin Assays, *Clin. Chem.*, **58**, 54–61 (2012).
219. Katrukha. A., Bereznikova. A., Filatov. V., and Esakova. T., Biochemical factors influencing measurement of cardiac troponin I in serum, *Clin. Chem. Lab. Med.*, **37**, 1091–1095 (1999).
220. Katus. H. A., Remppis. A., Scheffold. T., Diederich. K. W., and Kuebler. W., Intracellular compartmentation of cardiac troponin T and its release kinetics in patients with reperfused and nonreperfused myocardial infarction, *Am. J. Cardiol.*, **67**, 1360–1367 (1991).
221. Katrukha. A. G., Bereznikova. A. V., Esakova. T. V., Pettersson. K., Lövgren. T., Severina. M. E., Pulkki. K., Vuopio-Pulkki. L. M., and Gusev. N. B., Troponin I is released in bloodstream of patients with acute myocardial infarction not in free form but as complex, *Clin. Chem.*, **43**, 1379–1385 (1997).
222. "Cardiac troponin I Booklet", https://hytest.fi/resources/technotes/cardiac-troponin-i-booklet. Accessed03/2023.
223. Collinson. P. O., Heung. Y. M., Gaze. D., Boa. F., Senior. R., Christenson. R., and Apple. F. S., Influence of Population Selection on the 99th Percentile Reference Value for Cardiac Troponin Assays, *Clin. Chem.*, **58**, 219–225 (2012).

224. Apple. F. S., A New Season for Cardiac Troponin Assays: It's Time to Keep a Scorecard, *Clin. Chem.*, **55**, 1303–1306 (2009).
225. "How to use high-sensitivity cardiac troponin assays in everyday clinical practice", In *Troponin: Informative Diagnostic Marker – Nova Science Publishers*, Human Anatomy and Physiology, Nova Science Publishers, 61–71 (April 2014).
226. Mueller. C., Biomarkers and acute coronary syndromes: an update, *Eur. Heart J.*, **35**, 552–556 (2014).
227. Reichlin. T., Twerenbold. R., Reiter. M., Steuer. S., Bassetti. S., Balmelli. C., Winkler. K., Kurz. S., Stelzig. C., Freese. M., Drexler. B., Haaf. P., Zellweger. C., Osswald. S., and Mueller. C., Introduction of High-sensitivity Troponin Assays: Impact on Myocardial Infarction Incidence and Prognosis, *Am. J. Med.*, **125**, 1205-1213.e1 (2012).
228. Mueller. C., Giannitsis. E., Möckel. M., Huber. K., Mair. J., Plebani. M., Thygesen. K., Jaffe. A. S., Lindahl. B., and the Biomarker Study Group of the ESC Acute Cardiovascular Care Association, Rapid rule out of acute myocardial infarction: novel biomarker-based strategies, *Eur. Heart J. Acute Cardiovasc. Care*, **6**, 218–222 (2017).
229. Collinson. P. O., Saenger. A. K., Apple. F. S., and C-Cb. on behalf of the I., High sensitivity, contemporary and point-of-care cardiac troponin assays: educational aids developed by the IFCC Committee on Clinical Application of Cardiac Bio-Markers, *Clin. Chem. Lab. Med. CCLM*, **57**, 623–632 (2019).
230. Pickering. J. W., Young. J. M., George. P. M., Watson. A. S., Aldous. S. J., Troughton. R. W., Pemberton. C. J., Richards. A. M., Cullen. L. A., and Than. M. P., Validity of a Novel Point-of-Care Troponin Assay for Single-Test Rule-Out of Acute Myocardial Infarction, *JAMA Cardiol.*, **3**, 1108–1112 (2018).
231. Regan. B., O'Kennedy. R., and Collins. D., Point-of-Care Compatibility of Ultra-Sensitive Detection Techniques for the Cardiac Biomarker Troponin I-Challenges and Potential Value, *Biosensors*, **8**, 114 (2018).
232. WMA - The World Medical Association-WMA Declaration of Helsinki – Ethical Principles for Medical Research Involving Human Subjects (n.d.).
233. Brandmeier. J. C., Raiko. K., Farka. Z., Peltomaa. R., Mickert. M. J., Hlaváček. A., Skládal. P., Soukka. T., and Gorris. H. H., Effect of Particle Size and Surface Chemistry of Photon-Upconversion Nanoparticles on Analog and Digital Immunoassays for Cardiac Troponin, *Adv. Healthc. Mater.*, **10**, 2100506 (2021).
234. Raiko. K., Lyytikäinen. A., Ekman. M., Nokelainen. A., Lahtinen. S., and Soukka. T., Supersensitive photon upconversion based immunoassay for detection of cardiac troponin I in human plasma, *Clin. Chim. Acta Int. J. Clin. Chem.*, **523**, 380–385 (2021).
235. Long. G. L. and Winefordner. J. D., Limit of detection. A closer look at the IUPAC definition, *Anal. Chem.*, **55**, 712A-724A (1983).
236. Christenson. R. H., Jacobs. E., Uettwiller-Geiger. D., Estey. M. P., Lewandrowski. K., Koshy. T. I., Kupfer. K., Li. Y., and Wesenberg. J. C., Comparison of 13 Commercially Available Cardiac Troponin Assays in a Multicenter North American Study, *J. Appl. Lab. Med.*, **1**, 544–561 (2017).
237. Palamalai. V., Murakami. M. M., and Apple. F. S., Diagnostic performance of four point of care cardiac troponin I assays to rule in and rule out acute myocardial infarction, *Clin. Biochem.*, **46**, 1631–1635 (2013).
238. Collinson. P., Cardiac biomarker measurement by point of care testing - Development, rationale, current state and future developments, *Clin. Chim. Acta Int. J. Clin. Chem.*, **508**, 234–239 (2020).

239. Peeling. R. W., Holmes. K. K., Mabey. D., and Ronald. A., Rapid tests for sexually transmitted infections (STIs): the way forward, *Sex. Transm. Infect.*, **82**, v1–v6 (2006).
240. Otoo. J. A. and Schlappi. T. S., REASSURED Multiplex Diagnostics: A Critical Review and Forecast, *Biosensors*, **12**, 124 (2022).
241. Kettler. H., White. K., Hawkes. S. J., and Diseases. U. B. S. P. for R. and T. in T., *Mapping the Landscape of Diagnostics for Sexually Transmitted Infections : Key Findings and Recommendations*, World Health Organization (2004).

TURUN
YLIOPISTO
UNIVERSITY
OF TURKU

Painosalama, Turku, Finland 2023

ISBN 978-951-29-9385-7 Print
ISBN 978-951-29-9386-4 PDF
ISSN 2736-9390 (Painettu/Print)
ISSN 2736-9684 (Sähköinen/Online)